AD

USAAVLABS TECHNICAL REPORT 69-12

ADVANCED HIGH-SPEED FUEL PUMPS FOR SMALL GAS-TURBINE ENGINES

By

Harry T. Johnson

Robert K. Mitchell

April 1969

U. S. ARMY AVIATION MATERIEL LABORATORIES

FORT EUSTIS, VIRGINIA

CONTRACT DAAJ02-67-C-0037

BATTELLE MEMORIAL INSTITUTE

COLUMBUS LABORATORIES

COLUMBUS, OHIO

Disclaimers

The findings in this report are not to be construed as an official Department of the Army position unless so designated by other authorized documents.

When Government drawings, specifications, or other data are used for any purpose other than in connection with a definitely related Government procurement operation, the United States Government thereby incurs no responsibility nor any obligation whatsoever; and the fact that the Government may have formulated, furnished, or in any way supplied the said drawings, specifications, or other data is not to be regarded by implication or otherwise as in any manner licensing the holder or any other person or corporation, or conveying any rights or permission, to manufacture, use, or sell any patented invention that may in any way be related thereto.

Disposition Instructions

Destroy this report when no longer needed. Do not return it to the originator.

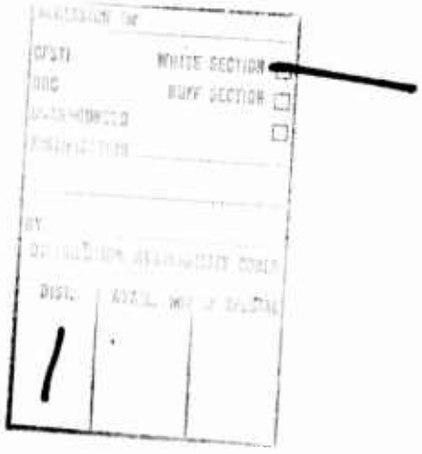

DEPARTMENT OF THE ARMY
U. S. ARMY AVIATION MATERIEL LABORATORIES
FORT EUSTIS, VIRGINIA 23604

The research described herein, which was conducted by Battelle Memorial Institute, was performed under U. S. Army Contract DAAJ02-67-C-0037. The work was performed under the technical management of Mr. R. G. Furgurson, Propulsion Division, U. S. Army Aviation Materiel Laboratories.

Appropriate technical personnel of this Command have reviewed this report and concur with the conclusions contained herein.

The findings and recommendations outlined herein will be considered in planning any future programs of high-speed pump development.

Task 1G162203D14416
Contract DAAJ02-67-C-0037
USAAVLABS Technical Report 69-12
April 1969

ADVANCED HIGH-SPEED FUEL PUMPS FOR SMALL GAS-TURBINE ENGINES

Final Report

by

Harry T. Johnson
Robert K. Mitchell

Prepared by

Battelle Memorial Institute
Columbus Laboratories
Columbus, Ohio

for

U. S. ARMY AVIATION MATERIEL LABORATORIES
FORT EUSTIS, VIRGINIA

SUMMARY

The object of this program was to develop the technology necessary for vane-pump operation at turbine rotational speeds. Major hardware emphasis was devoted to the evaluation of a high-speed fuel pump based upon this technology. A single-lobe vane pump with a centrifugal charging stage has been designed and successfully operated at 40,000 rpm pumping JP-4 turbine fuel. The vane pump relies upon the use of a hydrodynamically lubricated pivoting vane tip to support vane assembly radial loading. The hydrodynamic film allows a significant increase in tip surface speed without sacrificing the required endurance life. A 200-hour endurance run at speeds from 24,000 to 40,000 rpm has been successfully completed with no noticeable performance degradation. Successful contamination experiments were performed after completion of 175 hours of the endurance schedule. The contamination experiments were not extensive, but they verified that the design concepts were not unduly sensitive to contaminated fuel. Continued development will be required to establish life capability at the design pressure of 650 psig, but short-term capability has been established at outlet pressures up to 600 psig. No major limitations with the basic pump design have been found. The 50,000-rpm goal appears to be feasible, but further evaluation at speeds above 40,000 rpm was terminated due to bearing problems in the laboratory speed-increaser system.

TABLE OF CONTENTS

LIST OF ILLUSTRATIONS

LIST OF TABLES

BLANK PAGE

INTRODUCTION

Recent advances in the field of small gas-turbine engines have made possible a considerable reduction in the specific weight and volume of basic engine components. The field of engine-mounted accessories, however, has not produced comparable state-of-the-art advances. This is particularly true for advanced-design small engines in the airflow range of 10 pounds per second and less. Recent studies have indicated, however, that considerable improvement can also be made in this area of engine accessories.

The maximum allowable rotational speeds for present driven accessories, such as fluid pumps, make mechanical speed reduction necessary to transmit power from the higher speed turbines to these accessories. Elimination of the accessory drive gear-box, by driving all accessories at engine rotational speed, would result in a significant improvement in accessory system weight, volume, and complexity. Even if this is not entirely possible for certain very high-speed engines, increasing the rotational speed of the accessories would represent a significant advancement.

This report covers effort that was directed toward the development of high-speed capability for engine-driven fluid pumps, with major emphasis on the fuel pump. This report covers the time period from May 11, 1967, to November 15, 1968, and describes the design, fabrication, laboratory evaluation, and endurance evaluation of a high-speed fuel pump. In addition, some contaminated fuel evaluations were also accomplished.

Also considered from a theoretical standpoint were other aspects as related to the high-speed fuel-pump design. These included packaging considerations and emulsified fuels, and the feasibility of hydraulic and lubrication pumps of similar design.

DISCUSSION OF RESEARCH

OBJECTIVE

The basic objective of this program was the development of technology which would make the operation of positive-displacement fluid pumps at turbine engine rotational speeds practical. It is also fundamental that this technology be compatible with the use of low-viscosity fluids such as JP-4 turbine fuel without sacrificing the required endurance life of the pump elements. For design purposes, the development of a fuel pump capable of rotational speeds in the 30,000- to 50,000-rpm range was chosen as the primary goal of the program. The hypothetical operational requirements are noted in Table I.

TABLE I. FUEL PUMP REQUIREMENTS	
Maximum speed:	50,000 rpm
Maximum fuel flow:	750 lb/hr
Light-off fuel flow:	185 lb/hr at 6000 rpm
Design fuel pressure at 100% speed:	650 psig
Light-off fuel pressure:	200 psig
Maximum overpressure capability:	900 psig
Fuel:	MIL-F-5624 (JP-4 and JP-5) or MIL-F-46005A (CITE)
Fuel inlet temperature:	-65°F to +135°F
Fuel inlet pressure:	5 psi above true vapor pressure of the fuel
Maximum vapor/liquid ratio at inlet:	0.40

In addition to the above, the fuel pump development was to take into consideration the following objectives:

1. Pump configurations which will have low contamination sensitivity.

2. Pump configurations which demonstrate the feasibility of cartridge construction.

FUEL PUMP DESIGN

Design Considerations

Based on earlier work done at Battelle's Columbus Laboratories in high-speed pumps[1,2,3], a vane-type pump was chosen as the configuration which appeared to have the most promise in achieving a high rotational speed. A conventional vane pump is limited at high rotational speeds due to the contact between the vane tip and the cam ring. The boundary lubrication characteristic of this operation potentially allows accelerated wear of the vane tip at high tip surface speeds even when extremely hard materials are used. To avoid this limitation, a pivoting vane tip concept (Figure 1) has been developed which

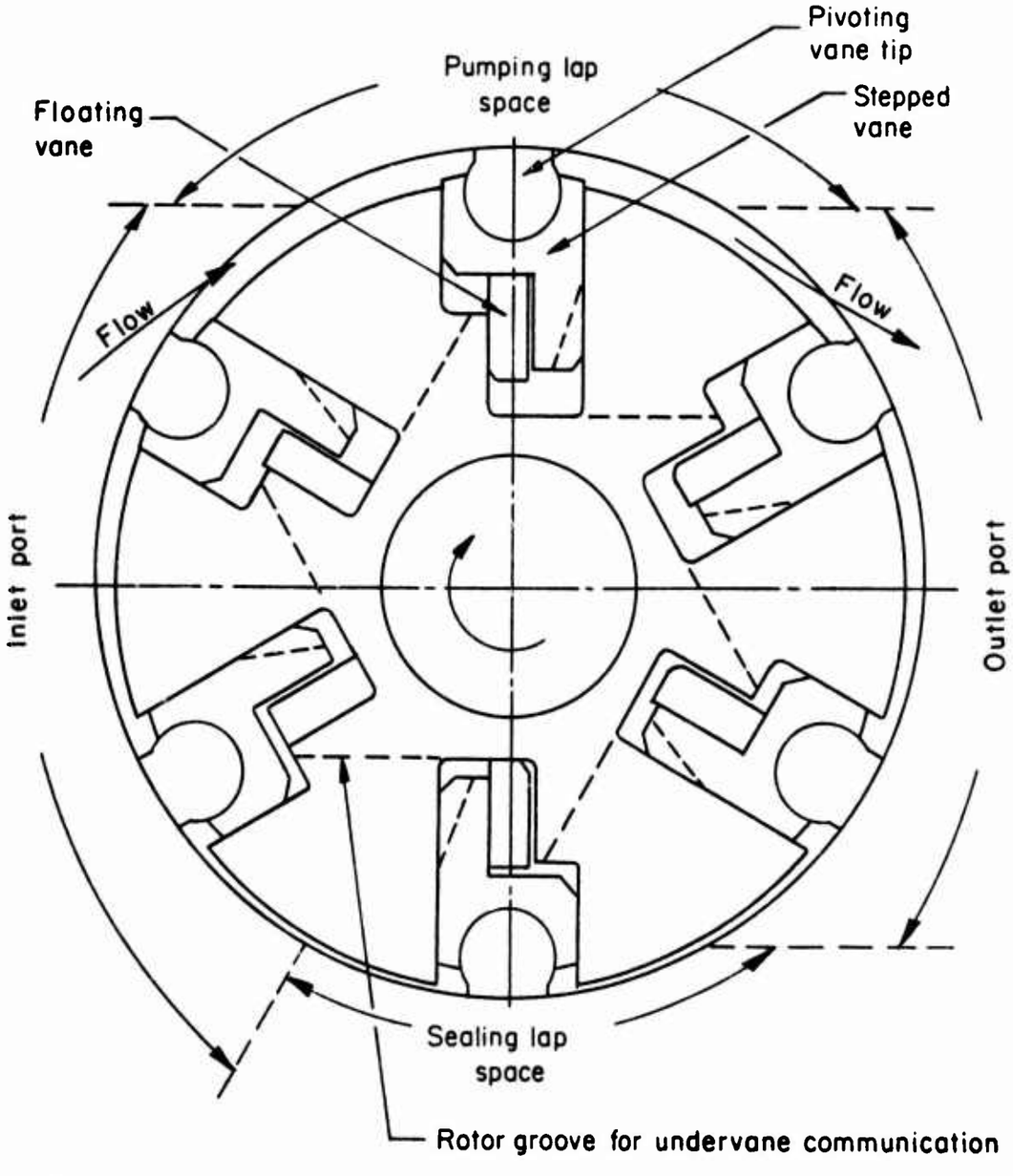

Figure 1. Fuel-Pump Rotor Cross Section.

relies upon hydrodynamic lubrication to support the vane centrifugal loading. The pivoting vane tip acts as a pivoted pad thrust bearing and the hydrodynamically generated film supports all radial vane loading. This allows higher tip surface speeds without reducing the life of the pump.

The high rotational speeds require that the inlet pressure to the vane pump be much higher than required by a conventional fuel pump system. Higher inlet pressure is necessary to accelerate the fuel to the high vane tip speed in the pump. To achieve this acceleration, a centrifugal charging stage has been designed which is capable of accepting a low inlet pressure at high rotational speed. The charging stage was made a centrifugal pump because this conventional approach had a high probability of success and allowed a greater effort to be placed in the design of the vane pump stage.

A fixed-displacement vane pump stage was chosen as opposed to a variable-displacement pump. Previous work at Battelle's Columbus Laboratories has indicated the feasibility of a flexible cam ring concept which allows for variable displacement. This, however, leads to some difficult and expensive fabrication techniques which would detract from the main objective of this program.

The early design work indicated that a two-lobe vane pump configuration was preferred because radial hydrostatic balancing of the rotor was achieved. This balancing produced low radial bearing loads and reduced fatigue loading on the rotor assembly. Further work in the design of the cam ring profile and the theoretical load-carrying capability of the pivoting vane tip with low-viscosity fluids indicated that a compromise was necessary to achieve high rotational speeds. It was found that a single-lobe cam ring profile permitted optimization of the load-carrying ability of the vane tip and therefore provided the greatest probability of success in achieving high surface speeds. Although a single-lobe vane pump stage would not produce radial rotor balance, it was decided that such a stage should form the basis for further design effort in order to obtain the optimum vane tip load support.

During the initial analysis of possible fuel pump configurations, a number of pump parameters were evaluated to determine their effect on the overall design. The parameters were weighted according to their importance in meeting the basic objective of high-speed performance. In some areas, compromises were made in an attempt to increase the probability of meeting the basic objective. Listed below are the parameters, their effect on the design, the necessary compromises, and the physical size requirements.

Rotor Diameter - Effect on Overall Design

1. Because the required vane pump stage inlet pressure is proportional to the square of the rotor diameter, a smaller diameter allows most of the developed pump head to be produced by the higher efficiency vane pump stage. It permits a single-stage centrifugal pump to be used to develop the required charging pressure.

2. Minimization of the rotor diameter allows for a relatively small total pump envelope.

3. A smaller rotor diameter reduces the vane tip surface speed and the centrifugal loading of the vane assembly, thereby helping to minimize the fluid heating in the area of the vane tip. The reduced fluid heating allows for increased performance from the hydrodynamic vane tip.

4. The size is limited structurally, so that the advantages listed above must be compromised to produce adequate rotor strength.

Vane and Vane Tip Assembly - Structural Considerations

1. Due to the low viscosity of turbine fuels, the hydrodynamic load support capacity of a pivoting tip is low. To insure non-contacting tip operation, it is necessary to minimize the centrifugal loading of the vane assembly that the tip is required to support.

2. To achieve this proper balance between load and load support, it is necessary to consider the use of low-density materials. Again, the structural requirements must be met. The vane strength requirements are minimized by using a small vane stroke, which transmits the major portion of the pressure loads to the rotor.

3. Due to the small stroke required to obtain the necessary fluid flow at high rotational speed, it is not necessary to encapsulate the pivoting vane tip in a vane socket. The removal of the socket requirements allows for a lighter assembly and a decrease in rotor size. The wear capabilities during stroking of the assembly are reduced, however, and for this reason the additional weight of the encapsulating socket technique was accepted to insure reasonable life in this area.

Cam Ring - Profile Configuration

1. Because of the complications involved in obtaining complete side-to-side hydrostatic vane balance when the vanes are subjected to a pressure differential on the pumping and sealing lap spaces (Figure 1), it was determined that the cam profile should not permit vane stroking in these areas. High frictional drag produced by the pressure differential would produce high vane tip loads when the vane is stroking radially inward and might cause vane lift-off if the centrifugal loading is not sufficient when the vane is stroking radially outward.

2. The profile must provide a continuously tangent path for proper operation of the vane tip bearing and have the variation in its radius of curvature bounded so that proper match with the tip radius can be achieved for all operating vane positions. The matching of the radii is necessary to provide sufficient tip load support for noncontacting operation.

3. It is advantageous to have a large stroking transition angle for the inlet and outlet ports to minimize the vane stroking velocity to help reduce wear on the sides of the vanes.

Hydrodynamic Vane Tip

The pivoted pad bearing action of the vane tip is required to support the entire centrifugal load of the vane assembly and any radially outward pressure loading due to communication of pump outlet pressure to the undervane area. With the low-viscosity turbine fuels (kinematic viscosity = 0.8 centistokes at 80°F), it is necessary to optimize the bearing load support to insure that the hydrodynamic film is not dissipated, thereby allowing high-speed contact with the cam ring. The bearing width and the match between tip bearing radius and the cam ring radius are the basic parameters that determine the load capability for fluid of a given viscosity. Although increasing the bearing width (circumferential dimension) does increase load support, it makes a good match with the cam ring more difficult to obtain and increases the mass of the vane assembly. Therefore, compromises must be made which affect many other parameters in the pump design.

Final Pump Configuration

Shown in Figure 2 is a layout of the final laboratory version of the complete fuel pump. Figure 1 gives the detailed rotor cross section,

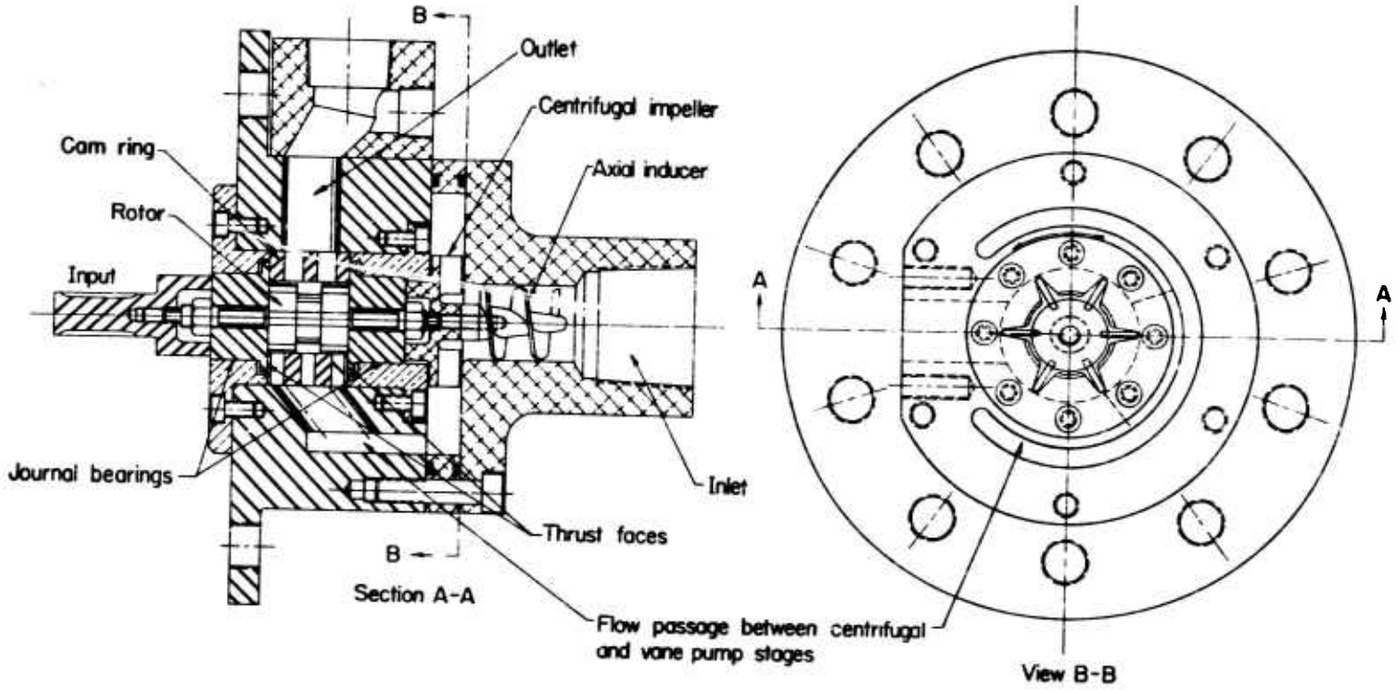

Figure 2. Fuel-Pump Assembly.

while Figure 3 shows an exploded view of the actual pump components. Table II gives the physical size of the overall pump and the individual pump parts in addition to the pump's theoretical capacity. This configuration represents the "C" revision, single-lobe version of the pump. Revisions "A" and "B" of the pump had the same centrifugal stage, pump body, bearings, and cam ring, with the major changes being incorporated in the design of the rotor and vane assembly in the vane pump stage. These revisions are shown in Figure 4. A layout of a two-lobe vane pump stage configuration was also made, but the inability of the two-lobe cam profile to supply the proper operating conditions for the hydrodynamic pivoting tip bearing limited this configuration's theoretical high-speed capability. Because of this, all further work was devoted to the development of a single-lobe vane pump stage for which 50,000-rpm capability was theoretically predicted without having to rely upon boundary lubrication of the vane tips. The packaging concepts and the centrifugal stage design of the two-lobe version were carried over to the single-lobe configuration, but additional work in bearing design was necessary to accept the high journal bearing loads imposed by a radially unbalanced single-lobe vane pump.

TABLE II. PUMP PHYSICAL SIZE

Theoretical capacity:	0.026 $in.^3$/rev
Number of vanes:	6
Vane stroke:	0.020 in.
Rotor diameter:	0.596 in.
Rotor axial length:	0.661 in.
Vane width:	0.110 in.
Vane tip socket diameter:	0.070 in.
Centrifugal impeller diameter:	1.12 in.
Axial inducer diameter:	0.63 in.
Journal bearing diameter:	0.75 in.
Basic pump envelope:	1.876 in. diameter by 3.0 in. long
Experimental pump envelope:	3.12 in. diameter by 3.7 in. long

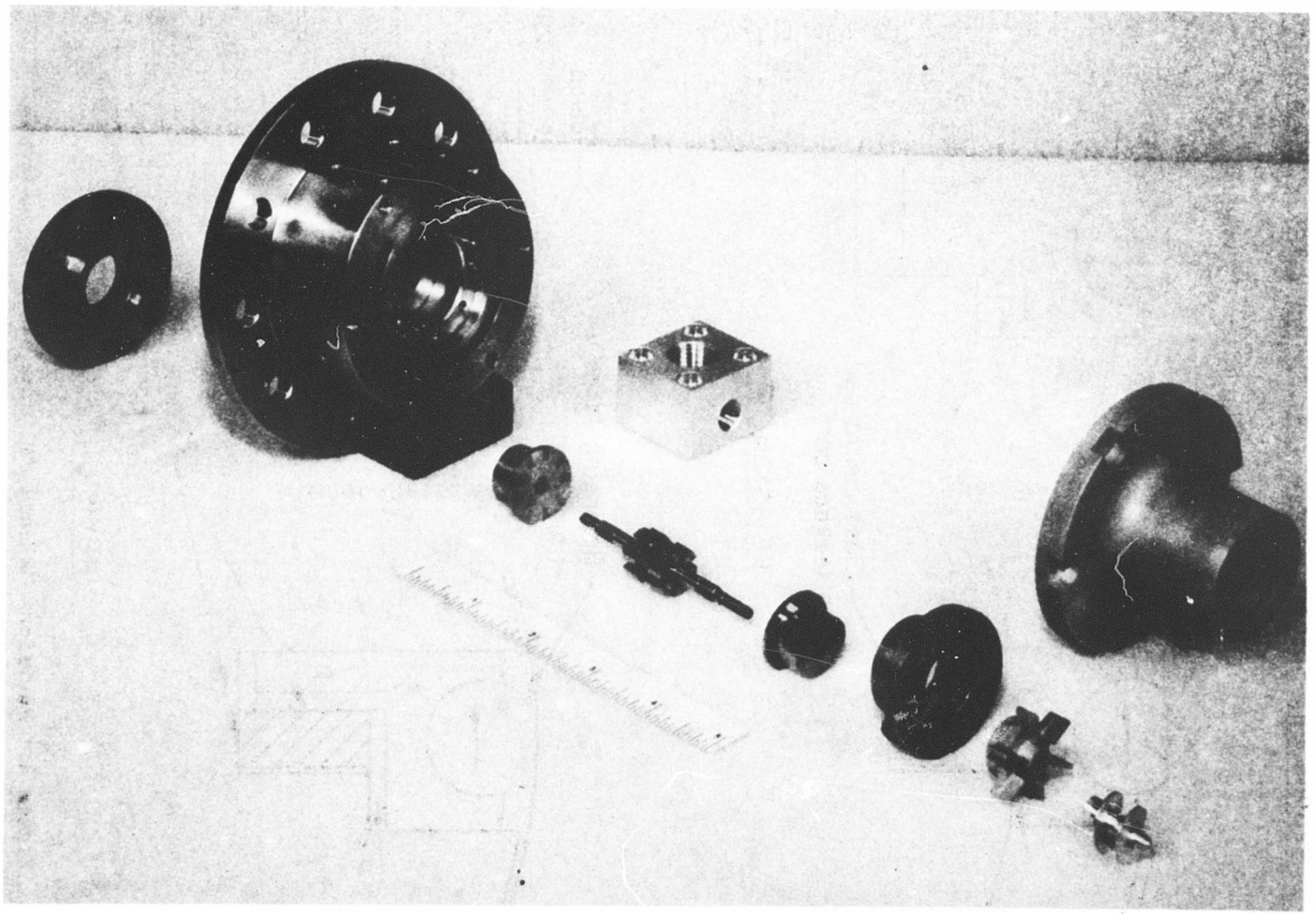

Figure 3. Exploded View Of Fuel-Pump Components.

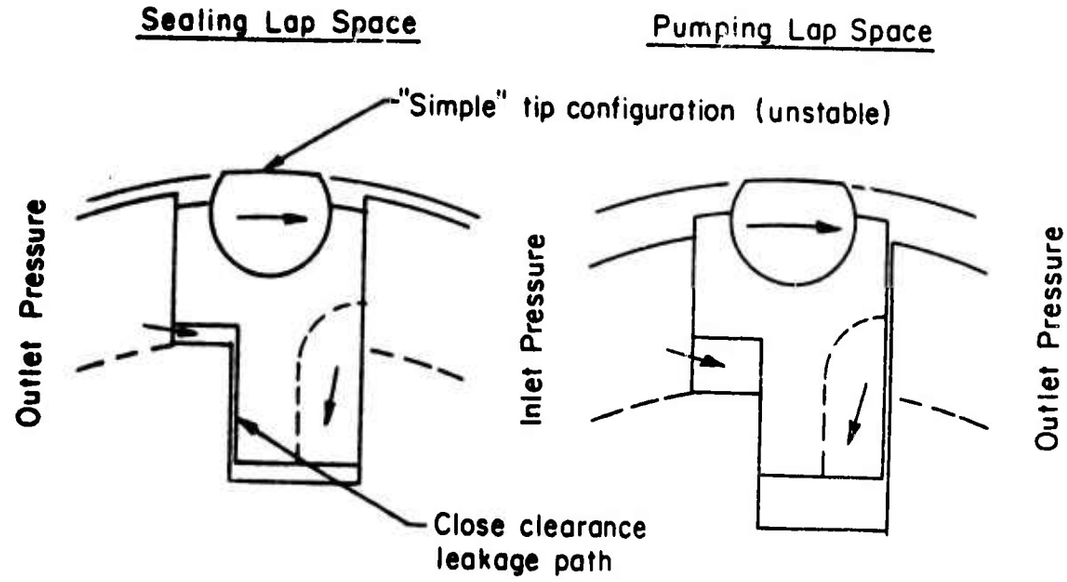

REVISION "A"

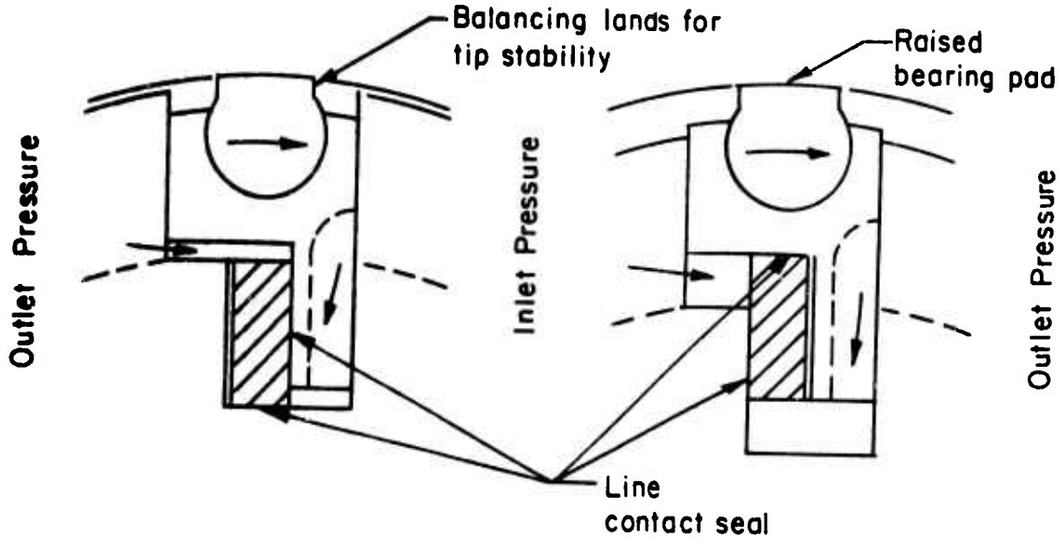

REVISION "B"

Figure 4. Revisions "A" and "B" Vane Assembly Designs.

The final pump design is actually a three-stage pump. The vane pump stage develops the major portion of the pump head. The centrifugal stage, cantilevered on the pump shaft opposite the drive end, provides the necessary charging pressure for the vane pump. In series with the centrifugal stage is an axial flow inducer which operates at the high levels of suction specific speed necessary to meet the low inlet pressure and high rotational speed conditions of the fuel pump. The axial inducer suppresses the cavitation level at the inlet to the centrifugal pump so that the centrifugal pump head is not radically reduced when operating at low inlet pressure, high vapor/liquid ratio conditions.

Vane Tip Design

The basic concept which achieves high vane tip surface speeds without sacrificing pump life is the pivoting vane tip. Its action as a hydrodynamic pivoted pad thrust bearing generates a fluid film between the tip and cam ring. Also, the operating film thicknesses between the tip and cam ring are still small enough (less than 100 μin.) that it provides a satisfactory seal when the vane assembly is subjected to a pressure differential. To analyze the capabilities of this concept, a computer program was used that was developed for this purpose in conjunction with previous Battelle efforts on high-speed hydraulic vane pumps. It predicted a minimum operating film thickness of 30 μin. at 50,000 rpm pumping JP-4 fuel. The surface finish required on the tip bearing and the cam ring surfaces to allow this operation are of a precision level, but well within the range of present-day machining capabilities.

A comparison of the two vane tip designs in Figure 4 reveals a change in the tip that was indicated during the initial testing of the pump with a pressure differential across the vane pump stage at low speeds. The revision "B" tip has the bearing pad surface raised 0.012 inch, producing a vertical land on the leading and trailing edges of the tip. The function of these lands is to counteract the moments generated on the tip by hydrostatic pressures that tend to cause unstable tip rotation on the pumping and sealing lap spaces. Tip stability is required so that proper orientation of the bearing surface with the cam ring is maintained. Earlier computer simulations had indicated that these lands were not necessary for proper tip rotational balance because the hydrodynamic pressures generated by the tip bearing were sufficient to overcome the hydrostatic generated moments. This, however, was based upon a false assumption that the high-speed, high-pressure operating conditions were the most severe. Later computer simulations at the low-speed failure conditions with revision "A" parts indicated that the tip would be unstable.

At low speed, the tip hydrodynamic pressure forces are greatly reduced due to the greatly reduced vane assembly centrifugal forces and the corresponding larger operating film thicknesses. The larger hydrostatic pressure forces create moments that are not balanced by the small hydrodynamic moments, with the result being unstable tip rotation for a revision "A" tip. Further computer simulations predicted success for the revision "B" tip at all pump operating conditions. Although the revision "B" tip is more difficult to fabricate, further pump evaluations verified its contribution to tip stability at low speeds. A theoretical discussion of the pivoting tip concept and predicted performance is found in Appendix I.

Vane Design

The vane has a stepped configuration to provide proper radial balancing of the hydrostatic pressures acting on the vane in the pumping and sealing lap spaces. As indicated in Figure 1, pressure ahead of the vane is communicated to the deep rotor slot undervane area by a groove through the axial center of the rotor and a relief in the leading edge of the vane. Pressure behind the vane is communicated in a similar manner to the shallow rotor slot undervane area. In the revision "A" design, a seal between the two undervane areas was achieved by maintaining very close clearances between the vane and rotor slot. On the inlet and outlet ports, the vane is placed in a uniform hydrostatic field and automatically balanced while the vane centrifugal force is used to cause the assembly to track the cam ring properly. The initial undervane split chosen placed 67% of the vane width in the deep rotor slot, and this was predicted to provide proper radial balance on both lap spaces at 50,000 rpm and 900 psig.

The early failure of the revision "A" parts also indicated a deficiency in this part of the vane design. This failure and the computer simulation at the failure conditions pointed out that vane balance was not achieved at low speed. The simulation predicted that a radial unbalance occurred and had caused the vane assembly to be blown from contact with the cam ring on the pumping lap space. This also contributed to tip instability, because of the resultant large film thickness. It also indicated that the balance predicted at 50,000 rpm was not a hydrostatic pressure force balance, but that the high centrifugal loads were supplying the needed force to achieve the total balance. At low speed, the centrifugal loading, which is proportional to the square of speed, was not sufficient to compensate for the hydrostatic unbalance.

Further investigation showed that a single-piece stepped vane could achieve complete hydrostatic radial balance on one lap space only, with the other lap space having to rely on the centrifugal loading for proper balance. The low-speed requirements of the fuel pump prohibited a compromise of this sort. Increasing the mass of the vane assembly to permit low-speed operation would also be a poor compromise because of excessive centrifugal loads at the higher speed conditions. The vane tips would not be capable of supporting these loads in the port areas, and the high-speed capabilities would be definitely limited.

The solution to the above problem was a two-piece vane that produced two separate undervane splits, each providing balance for a given lap space. This configuration is revision "B" in Figure 4. The split in the stepped rotor slot produces the required pressure distribution for the pumping lap space, while the split on the stepped vane provides it for the sealing lap space. The floating vane is positioned on each lap space so that the proper percentage of undervane area is exposed to outlet pressure. This provides for a complete hydrostatic balance on both lap spaces which is independent of speed and therefore meets the necessary low-speed fuel pump operational requirements.

A theoretical discussion of the radial vane balance question is found in Appendix I in conjunction with the vane tip analysis.

It was also found that the floating vane of the two-piece configuration solved another important problem. The position assumed by the floating vane on the lap spaces produced a line-to-line contact seal between the undervane areas. This is indicated in Figure 4. This factor removes the need to maintain very close clearances to decrease the leakage rate at this point. The low-viscosity turbine fuels made it necessary to insure that the clearances in this area were approximately 0.0005 inch in the revision "A" design to maintain reasonable leakage rates. The floating vane seal essentially eliminates leakage, however, and relaxes the need for precision fabrication techniques that would have been required to insure minimum clearances.

Cam Ring Design

Because of the low viscosity of turbine fuels, the cam profile chosen must be carefully considered if the abilities of a pivoting vane tip are to be realized. The tip is charged with supporting the centrifugal loading of the vane and tip plus any chosen hydrostatic radial unbalance and the radial vane drag forces due to inward stroking of the vane. At 50,000 rpm, this

loading is high and requires that the tip load support be optimized at all vane positions during the pumping of turbine fuel. To insure this, calculations predicted that the cam ring radius of curvature could be permitted to vary only approximately 0.020 inch for a pump with a 0.6-inch basic rotor diameter.

To meet this requirement, the single-lobe cam ring profile shown in Figure 5 was designed. This profile is adaptable only to a single-lobe vane pump and was the motivating factor in the decision to change from a two-lobe design. The profile is unique in that it is constructed of only two radii which generate the entire surface. The pumping and sealing lap space radii are concentric with the rotor axis and therefore do not permit vane stroking in the lap spaces. The stroking transitions in the inlet and outlet ports are identical; 120 degrees is required to complete the full transition on each port. This leaves 60 degrees for the pumping and sealing lap spaces and requires at least six vanes to be used in the rotor to obtain a seal at all times on the lap spaces. The port areas are also generated by using the lap space radii as shown, and therefore the variation in the radius of curvature of the cam ring is bounded by the difference between them, which is the pump stroke. Any other curve in the ports would produce larger and smaller radii of curvature and would increase the total variation. This would make tip bearing profile to cam ring profile optimization very difficult.

Although a single-lobe configuration is not hydrostatically balanced and requires the bearings to support this unbalance, its ability to produce an optimized match with the tip bearing radius greatly increases the maximum theoretical speed. In addition, a single-lobe configuration allows a smaller rotor diameter to be used because fewer vanes are needed and makes the inlet and outlet porting arrangements simpler. The smaller rotor diameter benefits many other pump considerations as long as structural strength can be maintained.

The centrifugal force of the vane assembly is the only force which insures that the vane tip tracks the cam profile without lift-off during the inlet and outlet port stroking transitions. This is due to the fact that the individual pressures are communicated to the complete undervane area in each port, producing a theoretical hydrostatic balance. On the inlet port, the undervane pressure is likely to be less than the inlet pressure due to the outward stroke of the vane and the flow of fluid into the undervane area. This produces inward radial unbalance that the centrifugal vane loading must overcome to insure proper vane tracking. On the outlet port the reverse is true.

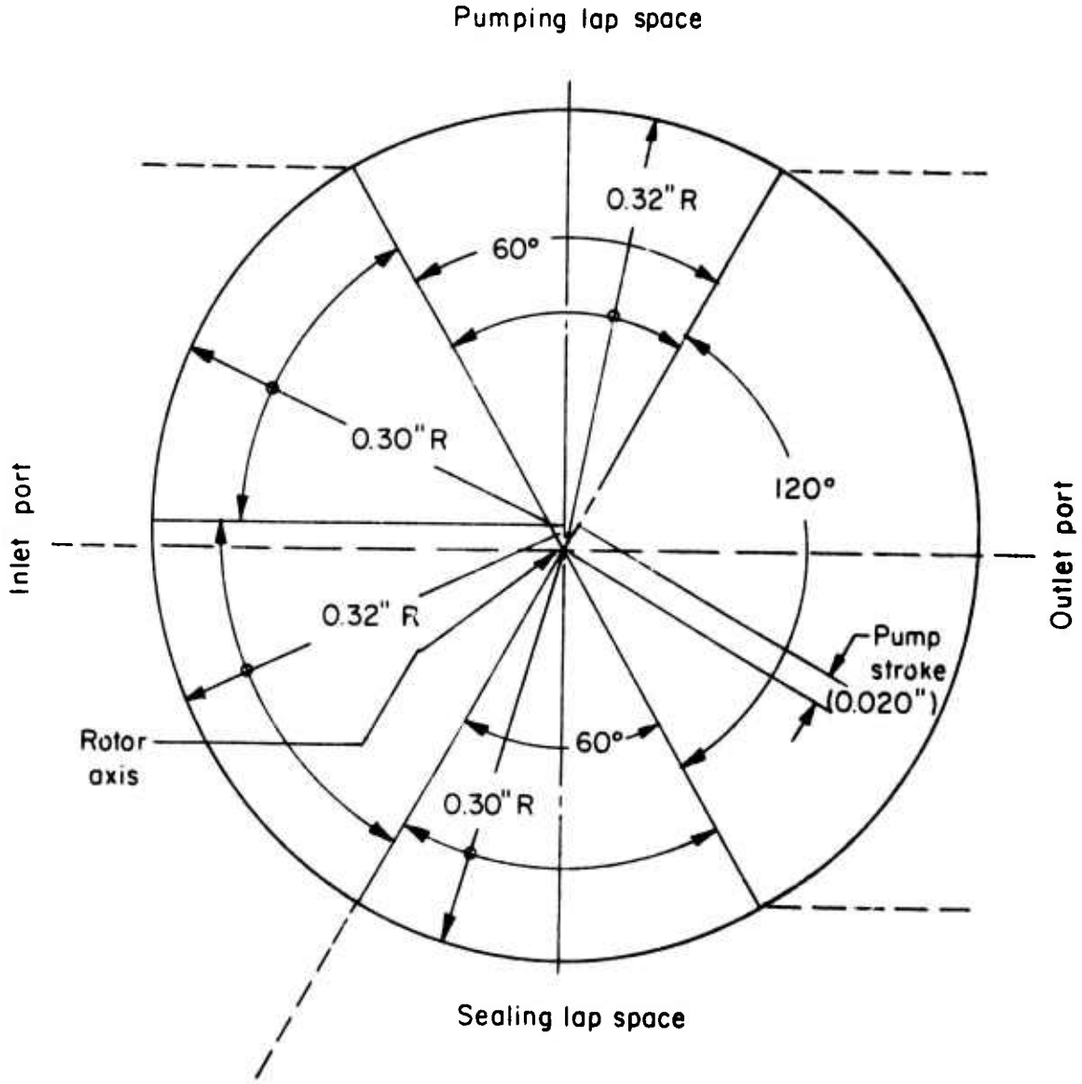

Figure 5. Cam-Ring Profile.

To maintain proper tracking under these conditions, the profile generated by the center of gravity of the vane assembly must be such that the center of curvature of the profile is always on the rotor side of the curve. The large stroke transition and small stroke of the cam profile in Figure 5 do an excellent job of insuring that the previous condition is met. The radius of curvature of the vane C.G. paths varies between 0.228 inch and 0.251 inch. It insures that the vane radial acceleration is always radially inward and that the fluctuations in its magnitude are minimized. Therefore, the cam ring profile provides sufficient centrifugal vane loading on the cam ring to produce proper vane tracking on the port transitions. This is particularly important on the inlet port, where the drag forces due to outward stroking and the slight reduction in undervane pressure would tend to cause the vane assembly to lift off.

Centrifugal Stage Design

Two types of centrifugal charging stages were designed and experimentally evaluated to determine their operational characteristics. A single-shrouded, backward-curved vane type and a fully open, radial vane type of impeller both proved to be capable of producing the required charging pressure and flow rate. The shrouded impeller created high axial thrust loads, however, and therefore the radial vane impeller was selected. The radial impeller not only minimized the thrust loading, but the radial vanes were structurally stronger and easier to fabricate. The original impeller was 1.5 inches in diameter, but this produced significantly more head than was needed to charge the vane pump stage. The final impeller is 1.12 inches in diameter and will produce approximately 300 psig at 50,000 rpm and design flow. This impeller, shown in Figure 2, has slightly improved efficiency and produces negligible axial thrust load due to the removal of all shrouding.

The axial inducer was designed using a trial-and-error experimental technique, due to the lack of basic theoretical information in this area. Although the 1.12-inch-diameter centrifugal impeller operates at inlet pressures near 10 psia, the addition of a single-pitch, 9.5-degree-pitch-angle axial inducer allows operation at 7 psia. The axial inducer suppresses the formation of cavitation at the impeller inlet, and therefore the centrifugal head is not significantly degraded at low inlet pressures.

The head developed by the centrifugal stage is more than the theoretical charging pressure required by a 0.6-inch-rotor diameter vane pump. The pressure required is approximately 100 to 120 psi at 50,000 rpm operation. It was felt that the additional charging pressure would provide a safety margin during the complete pump evaluation to insure that the expensive vane

pump stage parts would not be lost due to marginal centrifugal stage operation. This decision causes the final test version of the pump to be somewhat less efficient when operating at high speeds and the corresponding high centrifugal charging pressures. The centrifugal diffuser section has not been optimized. As a result, the recovery of the velocity head developed by the impeller is very poor. This partially accounts for the low efficiency level of the laboratory version centrifugal stage. The charging pressure developed is sufficient in spite of this, and the simple radial diffuser section made fabrication of the centrifugal stage relatively inexpensive.

Centrifugal impellers operating at the speed, head, and flow conditions required by the fuel pump (low specific speed centrifugals) are not highly efficient. In fact, low specific speed conditions are usually served best by positive displacement type pumps because of this low efficiency. It is very possible that the centrifugal stage has a maximum efficiency level of about 50 percent even if its design is optimized. No attempt was made to optimize the centrifugal stage, for it was felt that the major effort should be applied to the development of the vane pump stage. To improve the efficiency of the centrifugal stage, a better match between its flow capacity and that of the vane pump stage should be made.

Bearing Design

Due to the high speeds involved, it was decided to use journal bearings instead of antifriction type bearings to support the radial loading. The only lubrication available is from the turbine fuel being pumped. The fuel also makes the use of antifriction type bearings difficult unless they are grease lubricated and completely sealed from the fuel. Fuel-lubricated journal bearings, however, not only supply the necessary load support at high speed but also act as seals to prevent excessive pump leakage.

Hydrodynamic journal bearings were chosen in favor of hydrostatic bearings because the latter required greater leakage flow to maintain their load support. The plain journals shown in Figure 2 are very precise bearings, and close control of the bearing clearances and alignment was maintained during their fabrication. To provide the required hydrodynamic load support at all speeds and pressure conditions, a nominal diametral clearance of 0.0008 inch and a 0.75-inch journal diameter were required. The large diameter was necessary so that the load support could be achieved with shorter, more compact bearings.

Operation at -65°F would cause the 0.0008-inch clearance to be reduced to 0.0002 inch because of a poor thermal match between the journal and sleeve materials. For the experimental pump, this condition was accepted so that a sleeve material with a high level of conformability could be used.

To accept the centrifugal-generated axial thrust loads and to stabilize axial rotor motion at high speeds, two hydrodynamic thrust bearings were incorporated into the design. They are fuel-lubricated stepped thrust bearings and use the sides of the cam ring as a thrust surface as indicated in Figure 2. The stepped configuration shown in Figure 6 generates a hydrodynamic film that supports an axial thrust load. The two bearings act against each other to maintain axial rotor equilibrium. They support axial thrust loads in either direction and operate with a nominal film thickness of 500 μin. when unloaded. The nominal clearance is maintained by controlling the difference between the rotor and cam ring lengths. Each thrust bearing has a theoretical load capacity of 170 lbs at a 40-μin. film thickness.

The thrust bearings also require precision fabrication to insure proper operation. Because of the small film thicknesses involved, all surfaces must be extremely flat and parallel. Also, close control must be maintained over the step height of these bearings. The step height should be approximately 200 μin. to optimize the bearing performance.

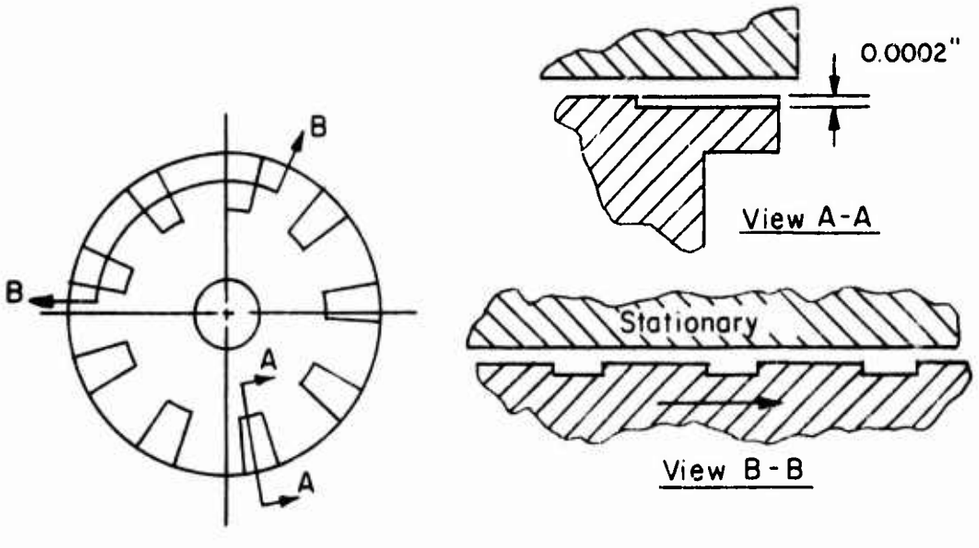

Figure 6. Stepped Thrust Bearing Configuration.

Rotor Assembly

The rotor and shaft are of one-piece construction. Two-piece construction would be preferable, but it was relinquished so that the rotor diameter could be minimized. The journals are clamped to the rotor and shaft by the nuts at each end of the shaft. These nuts are torqued to 25 in.-lbs to preload the assembly. The placement of the large-diameter journals in this manner produces a relatively strong rotor assembly, which is more capable of withstanding the radial load due to the hydrostatic unbalance of a single-lobe pump design. The preload, or initial tension in the shaft, is advantageous in reducing the fatigue effects of the cyclic side load. As in most fastener applications, the preload is used to reduce the variation in stress level. The fatigue effects, which depend on the extent of the variation of the stress, are correspondingly reduced. Fatigue is of prime concern due to the high number of revolutions or stress cycles the pump will experience durings its required life. The clamping action of the journals on the sides of the rotor is also beneficial, in that it helps to support the rotor segments when they are loaded by a vane exposed to a pressure differential.

The rotor and journal assembly configuration causes all thrust loads to be accepted on the sides of the cam ring as previously noted. The complete thrust face serves as a rotor end plate. The fact that these end plates rotate with the rotor is a deviation from conventional vane pump design, in which the end plates are normally stationary. This configuration is a result of the need for journal diameters which are larger than the rotor and of the thrust bearing performance improvements derived from placing a small area thrust runner at a larger diameter. The latter conditions detract from the pump mechanical efficiency because they require more power. The efficiency must be compromised, however, to produce the necessary load capabilities.

Because of the rotating end plates, there is no rotational relative motion between the ends of the vanes and the end plates. The only relative motion is due to the radial stroking of the vanes. This fact caused some concern about the ability of the vane to stroke without jamming on the ends. Early pump evaluations eliminated this concern, and it became apparent that jamming would not occur as long as the vane tracked the cam ring properly. The cam ring insures proper vane alignment with the end plates and eliminates the axial vane cocking necessary for jamming.

Vane Stage Porting

The radial porting of the vane pump stage is also a deviation from conventional vane pump design. Normally, vane pumps are ported axially. The small stroke (0.020 in.) and relatively long rotor length (0.66 in.) make this impractical. The radial porting produces a much more direct flow path to and from the vane pump stage. The fluid is not required to change direction radically, and therefore the theoretical internal flow losses are reduced. The large flow annulus from the centrifugal stage produces low fluid velocity between stages, and the resultant flow losses are also reduced in this area.

Pump Body Configuration

The pump body and the flow passages have been designed so that they demonstrate the feasibility of cartridge construction. The pump envelope shown in Figure 2 is larger than that required for cartridge construction so that the pump could be adapted easily to the existing Battelle test rig. The inlet and outlet manifolds also reflect this requirement in their configuration. The basic pump cartridge envelope falls within the flow annulus between the centrifugal stage and vane pump stage. If the flow passages were made a part of an overall accessory system structure, then the basic pump envelope would be 1.876 inches in diameter and approximately 3 inches long.

Pump Capacity

The pump was sized based on the light-off speed and fuel-flow conditions of 6000 rpm and 185 lb/hr. This sizing is necessary because of the low vane pump volumetric efficiency at the low flow conditions. The sizing is based on a theoretical volumetric efficiency of 69% at the light-off pressure. The resultant capacity is 0.026 $in.^3$/rev and includes complete undervane volume participation. A slight volumetric loss in the undervane capacity will take place due to the floating vane motion on the sealing lap space. This loss is due to physical undervane clearances required to fabricate parts with reasonable tolerances. This loss will reduce the theoretical capacity approximately 5%, but it is not the cause of the flow losses described in the pump evaluation section of this report. Those losses are due to an unexpected and unexplained motion of the floating vane in the inlet port segment of the pumping cycle.

Due to the fixed-displacement characteristic of the pump and its sizing at 6000-rpm conditions, the pump capacity at 50,000 rpm will greatly exceed the flow requirement of 750 lb/hr even when leakage losses are considered. The theoretical flow at this speed was calculated to be approximately 2150 lb/hr or 2.9 times the required flow. This fact points out the major disadvantage of a fixed-displacement fuel pump. The present fixed-displacement fuel pump therefore represents a compromise in this area. The decision to build a fixed-displacement pump in light of this was made in order to establish the requirements for high-speed operation with low-viscosity fluids. The addition of the variable-displacement problem would have clouded the primary objectives and delayed early hardware evaluation of the pump concepts.

Materials and Fabrication

Due to the high speed and the close clearances required for proper performance of the pump elements, many of the basic pump parts require precision machining techniques. This fact plus other design and pump environmental requirements makes the choice of materials very important. Table III lists each part and the materials used in the final laboratory version of the pump. It also gives a brief discussion of the factors considered in making the choice for each particular part.

TABLE III. PUMP COMPONENT MATERIALS

Part	Material	Comments
Cam Ring	"Ferro-Tic C", a powder metal composite of titanium carbide cemented by an alloy tool steel matrix. Hardness - 68 to 71 Rc.	Chosen because of its stability, resistance to galling or pickup, and low coefficient of friction. These properties are particularly important for high-speed thrust bearing performance and to insure that localized vane tip film breakdown or contact with the cam ring surface does not cause material transfer which would lead to self-destruction. It improves pump contamination resistance. "Ferro-Tic C",

TABLE III - continued

Part	Material	Comments
		in its annealed form, can be machined to form, then heat treated to obtain desired properties. This fact allows conventional fabrication techniques with short lead times.
Vane Tip	"Purebon" Grade P-5AG, a silver-impregnated carbon-graphite material. Shore scleroscope hardness of 90.	Chosen because of its self-lubricating and non-galling properties, and its low coefficient of friction, especially when a hydrodynamic film is maintained. These properties meet the requirements of the high-speed pivoting pad bearing concept used with the pivoting vane tip. The material is compatible with JP-4 fuel and has excellent corrosion resistance, even at high temperatures. Its low density (S.G. = 2.35) minimizes the centrifugal loading of the vane assembly. Contamination experiments have shown that it has marginal contamination resistance.
Stepped Vane	6061-T6 Aluminum	Low density (S.G. = 2.7) and resulting decrease in vane assembly centrifugal loading form the basic reason for choice. Not wear-resistant, but early wear patterns provided useful evidence of vane position during operation. Hard anodizing or ceramic

TABLE III - continued

Part	Material	Comments
		coatings would provide contamination resistance without a weight increase.
Floating Vane	6061-T6 Aluminum with a 0.001-inch-thick hard anodic coating	Low density (S.G. = 2.7) provides low centrifugal loading. The anodized surface provides wear and contamination resistance.
Combination Thrust Bearing and Journal	"Ferro-Tic C", Hardness - 68 to 71 Rc.	Same reasons as with the Cam Ring. The high hardness level provides an excellent journal material.
Sleeve Bearing	SAE 67 Leaded Bronze	Good embeddability, which allows it to absorb foreign particles; also, a high level of conformability, which allows it to compensate for misalignment and conform to geometric errors with a minimum of scoring and wear. The latter was important for the first experimental pump so that any marginal conditions would not produce major failures. High levels of contamination would probably require a harder material to minimize abrasive wear.
Rotor & Shaft	4340 Steel, Hardness - 40 to 45 Rc.	Chosen to obtain high strength in combination with toughness to minimize stress concentration effects.

TABLE III - continued

Part	Material	Comments
Centrifugal Impeller & Axial Inducer	6061-T6 Aluminum	The ease of machining aluminum makes the fabrication of the complex forms faster and less expensive. Allowed for quicker experimental evaluation and modification required to obtain a suitable design. Contamination and cavitation resistance could be improved by using ceramic coatings.
Vane Pump Stage Body	304 Stainless Steel	This part needed only for the experimental version of the pump. A cartridge configuration would take a completely different form.
Centrifugal Stage Cover & Spacer	6061-T6 Aluminum	Same as above

The vane pump stage parts were fabricated by Speedring Corporation in Warren, Michigan. They were responsible for the design of all tooling necessary to fabricate one complete set of pump parts. In addition, they submitted documented inspection reports on all critical part dimensions to insure that the drawing requirements were met. The centrifugal stage parts were fabricated in the machine shop of the Battelle Columbus Laboratories. The short lead time required for these parts, due to their less precise requirements, allowed them to be completely evaluated prior to the completion of the vane pump fabrication.

During the fabrication of the vane pump stage parts, close attention was given to the techniques used to build the journal bearings. Because of the close clearances required for both the journal and thrust bearings, the alignment of the journal bearings with each other and with respect to the thrust bearing is critical. Also, the alignment must be repeatedly maintained during each reassembly of the pump. To insure this, the following techniques were used:

1. The finish journal diameters were ground to size, concentric with each other and perpendicular to the thrust faces, as an assembly with the rotor and shaft.

2. To insure repeatability, the shaft diameters and the mating bore in the journals were matched with a maximum clearance of 50 μin. In addition, the angular position of the journals was indexed using etched reference marks.

3. The nut faces were match lapped to the corresponding journal faces to insure that the application of the torque to the nut did not distort the shaft axis.

4. The sleeve bearings were line bored under conditions that simulated the final assembly of the pump. They were lapped to size concentric with each other and perpendicular to one face of the cam ring. A spacer simulated the cam ring for this operation and was manufactured to tighter tolerances than those of the cam ring.

5. To insure repeatable assembly, each sleeve bearing was doweled to the pump body. The dowel holes in the sleeves were lapped to size so that a line-to-line fit with the pins was achieved. This was done prior to final sizing of the sleeve bores.

The care taken with the bearings allowed rotors fabricated at a later date to incorporate design modifications to be interchangeable with the original rotor.

The carbon-graphite tips used in the final version of the pump were of two-piece construction to simplify the machining operations. The bearing pad portion of the tip is bonded to the pivot section using a high temperature adhesive (Armstrong A-701). This adhesive produces an excellent, repeatable bond between carbon surfaces in addition to being compatible with JP-4 fuel. The pivot section was completed to finish dimensions prior to the bonding operation, but the bearing pad radius was generated as the final operation on the bonded assembly.

The revision "A" tips were each fabricated from a single piece of beryllium oxide. This material proved to be abrasive and caused wear in the aluminum vane socket during the preliminary pump evaluation. Fabrication was also started on an electroless, nickel-plated, 6061-T6 aluminum version of the tip. Though this technique seemed feasible, the parts were never completed due to the early success with the carbon version.

The original rotor was fabricated from A-2 tool steel, hardened to 60 Rc. It proved to be very sensitive to stress concentration in the thread areas, even though these areas were drawn back in hardness. To overcome this problem, the material was changed to 4340 steel and a special thread form was used. The thread form increased the thread root radius and lowered the stress concentration factor in this area. This thread form is normally used with brittle materials such as beryllium.

The cam ring is held in place by a light, 200-μin. interference fit with the pump body bore. This allows easy removal of the part by heating the assembly due to the difference in the thermal expansion rates of the two materials. It was found, however, that even this light interference fit caused distortion of the ends of the cam ring. These distortions affect the performance of the thrust bearings. The resulting problem due to the interference fit indicates that an adhesive bond would provide a better means of assembling these parts.

PERFORMANCE EVALUATION

Laboratory Equipment

A 10-hp motoring dynamometer was used to drive the experimental pump. The dynamometer has a maximum speed of 6000 rpm, so a speed increaser system was required. A 9.5/1 speed increase was achieved using the flat belt drive system shown in Figure 7. The high belt side loads required that a special support system be designed for the high-speed pulley. The driven pulley shaft is positioned and rolls on four large-diameter wheels. The result is that all bearings in the system rotate at much lower speeds, allowing the use of standard pillow blocks.

This system proved to be a durable and inexpensive way of driving the high-speed, low-power pump. The low power level required to drive this system at high speeds also allows a more accurate determination of the required pump input power.

The pump was directly driven through keys by an extension to the high-speed pulley. A shear pin type failure link was used in an attempt to minimize the effects of a pump failure or lockup. The keys were provided so that axial loading of the pump bearings by the speed increaser was limited. The drive shaft system was sized to place all critical shaft speeds above 50,000 rpm.

The pump was instrumented so that flow rate, inlet and outlet pressures, inlet and outlet temperatures, speed, and input power could all be monitored.

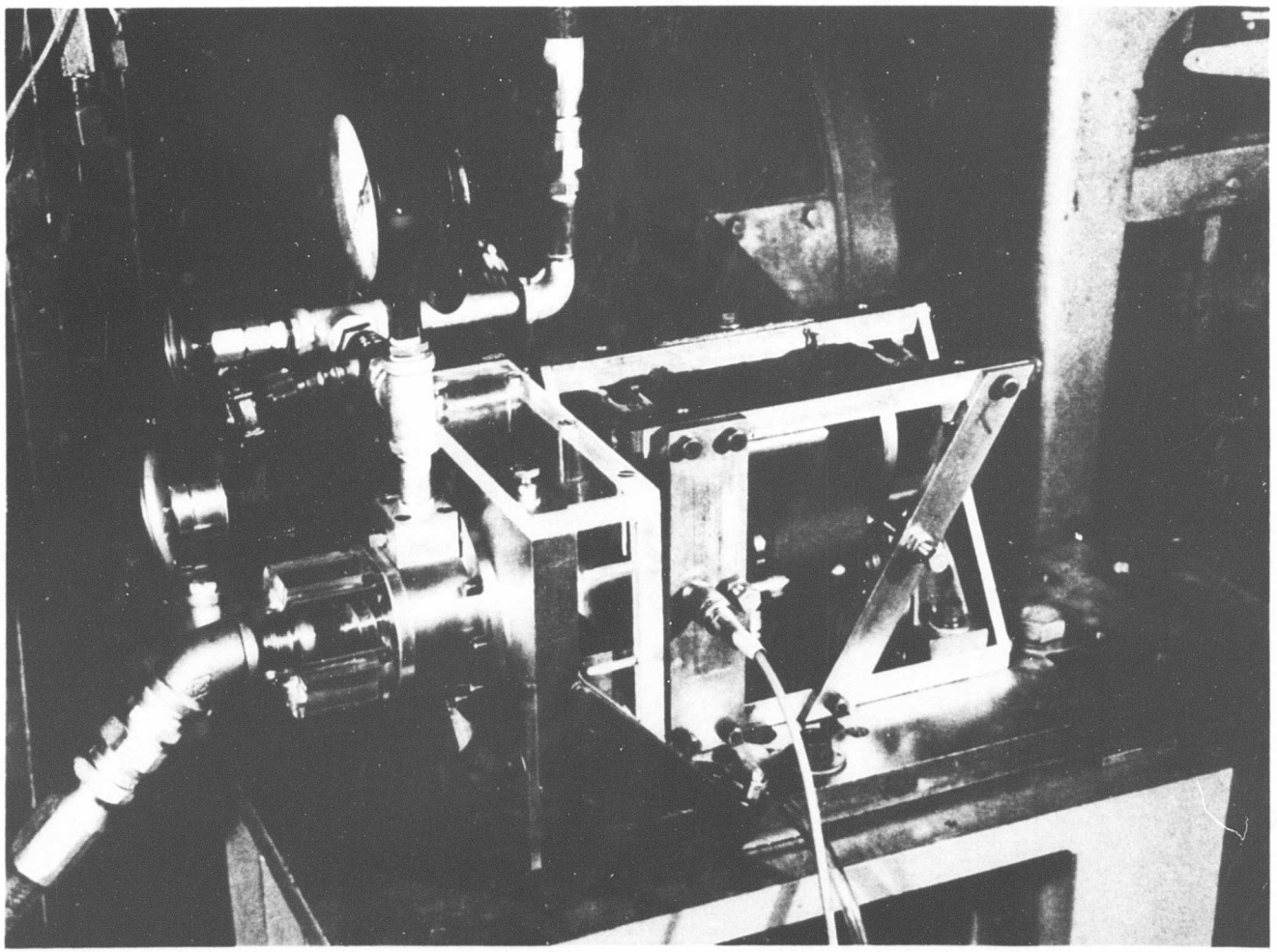

Figure 7. Experimental Fuel-Pump Evaluation Equipment.

The test fluid used for all of the experimental pump evaluation was JP-4 turbine fuel. The fuel was filtered so that all evaluation and endurance operation was performed with fluid essentially free of contaminant. The nominal fuel inlet temperature was approximately 50° to 75°F for all evaluation and endurance operation. The pump inlet pressure unless otherwise noted, was atmospheric.

Preliminary Evaluations

The performance characteristics of the centrifugal stage, including the axial inducer, were evaluated prior to the completion of the vane pump fabrication. The 1.12-inch-OD radial impeller was operated successfully with JP-4 fuel at speeds as high as 45,000 rpm with the inlet pressure reduced to 7 psia. This impeller produces sufficient charging pressure for the vane pump stage and does not produce large axial thrust loads. An earlier test with a 1.5-inch-OD shrouded impeller produced thrust loads large enough to overload the test rig thrust bearings and cause failure at 25,000 rpm.

The pressure-flow performance curve for the radial impeller is very flat. Figure 8 demonstrates this for operation at 25,000 rpm. The flow capability of the impeller also exceeds the required theoretical flow rate of the vane pump stage. This mismatch between the stages accounts to a large degree for the low centrifugal efficiency when operating with the vane pump stage. Restricting the centrifugal flow rate below the optimum capacity causes the centrifugal stage to operate at a very inefficient point on its performance curve. This is shown in Figure 8 for various flow rates.

The reduced inlet pressures were obtained by placing a throttling valve at the inlet to the centrifugal stage. A disadvantage of this technique was that the fuel cavitated as it passed through the valve and the resulting fuel entering the pump had a very high level of vapor. The vapor level was not measured, but operation under these conditions does indicate that the centrifugal stage can perform satisfactorily at high-vapor-content, low-inlet-pressure conditions.

The axial inducer operates in a cavitating regime at low inlet pressures without being completely choked. With a 9-psia inlet pressure, the centrifugal head is decreased by approximately 20 percent at 30,000 rpm. At 45,000 rpm, the inlet pressure can be reduced to 7 psia before a 20-percent reduction in head is obtained. Under these conditions, a stable cavitation ring forms at the ID of the centrifugal impeller, but the discharge fuel appears to be vapor free. In general, the ability of the axial inducer to suppress the cavitation level at the centrifugal inlet improved with increasing speed and flow rates. Continuous operation of the centrifugal stage at low inlet pressures did not cause any wear of the aluminum parts.

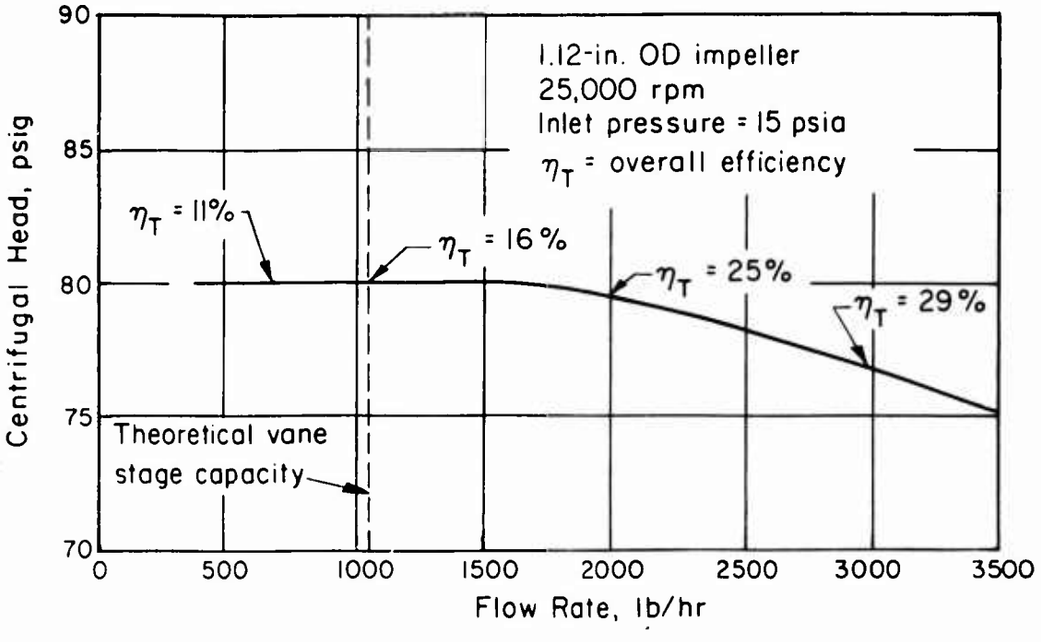

Figure 8. Centrifugal Stage Experimental Pressure - Flow Performance.

Prior to operation of the complete pump assembly, the speed capability of the bearings was established. The pump was assembled without vanes and vane tips using a modified rotor without vane slots and with a 0.38-inch rotor diameter. The centrifugal stage was used to supply flow to lubricate the bearings and to produce the actual operating thrust loads. The bearings were successfully operated at 40,000 rpm with no indication of marginal performance. This did not represent a speed limit, but further testing at higher speeds was delayed until total pump capability was demonstrated at 40,000 rpm. This evaluation also demonstrated the compatibility between the drive system and the pump at high speed.

The initial pump evaluation was performed using revision "A" vanes and vane tips. Successful operation was obtained at 25,000 rpm with a zero differential pressure across the vane pump stage. The zero pressure differential condition requires an outlet pressure of 80 psig which corresponds to the centrifugal charging pressure at this speed. The subsequent inspection of the cam ring revealed light axial polish marks on its surface in the areas of lowest tip load support capability. The physical inspection of the surface indicated that these polish marks corresponded to the removal of microinch surface

asperities in the 20-30 μin. range. The transition irregularities between the profile radii were also smoothed out considerably. The localized contact between asperities is to be expected at this speed, because film thicknesses in the 50-70 μin. range were theoretically predicted with perfect surfaces. The carbide cam ring and beryllium oxide tips were hard enough to accept this contact without galling and self-destruction and, therefore, were able to accept the run-in conditions without failure. To eliminate this type of run-in contact, it would be necessary to specify surface finishes lower than the 8-μin. center line average specified on the original parts. The above operation, however, served as a run-in which produced the more desirable operating surfaces.

The pump evaluation continued at 15,000 rpm with a pressure differential applied to the vane pump stage to obtain preliminary operating results as early in the program as possible. The pump failed at this speed when an outlet pressure of 150 psig was applied. The performance data at the time of failure, the subsequent inspection of parts, and a theoretical simulation of the failure conditions all indicated that the failure was due to vane and vane tip instability at the test conditions.

The preliminary evaluation indicated that the pivoting tip had the load support capability necessary for high-speed operation. The failure, however, pointed up deficiencies in the vane and tip design, and the changes incorporated in the revision "B" design reflect what was learned from this early evaluation.

Final Pump Evaluation

That the changes in the revision "B" vane assembly design improves vane and vane tip stability was verified by successful operation of the pump at design pressure for all speeds up to and including 30,000 rpm. The pressure envelope used was based on a linear pressure distribution from 6000 rpm, 200 psig to 50,000 rpm, 650 psig. In each case, the test conditions were maintained for 15 minutes. Successful operation at the 6000-rpm light-off condition is particularly encouraging, because the most severe stability requirements were predicted by the computer simulation for this operating point. In addition, it is also the condition at which marginal journal bearing operation was a possibility due to the low rotational speed and the resulting minimization of the bearing load support capabilities.

Figure 9 shows the flow rate performance curves for various operating conditions. The resulting volumetric efficiency is much lower than the theoretical predictions. At 25,000 rpm, 400 psig, the efficiency is only 68 percent whereas the predicted level would be approximately 90 percent. As a result of the reduced volumetric efficiency, the pump capacity of 115 lb/hr at 6000 rpm does not meet the required light-off fuel flow of 185 lb/hr.

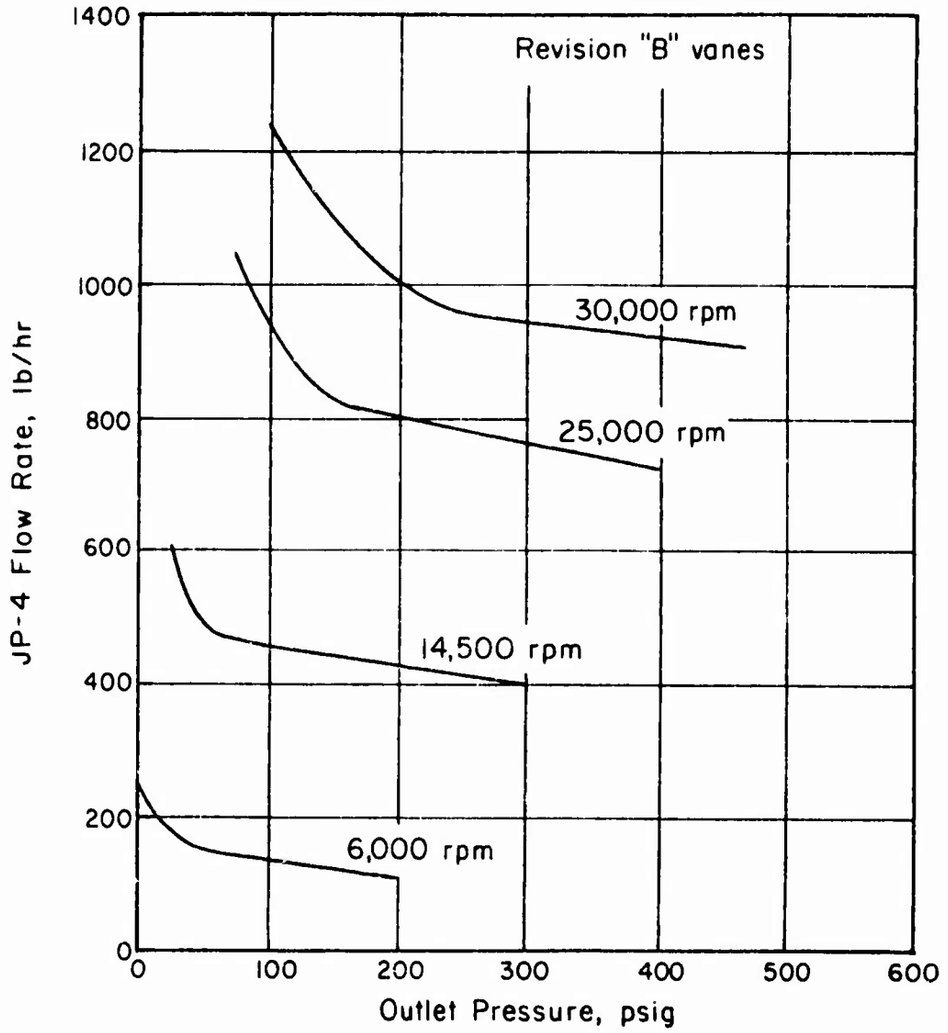

Figure 9. Experimental Flow-Rate Performance, Revision "B" Fuel-Pump Configuration.

The pump capacity with a zero pressure differential across the vane pump stage correlates well with the theoretical pump capacity at each speed. It is slightly less than predicted, but the leakage past the bearings due to the centrifugal charging pressure accounts for the deviation. The unusual shape of the flow rate performance curves, however, suggests that more than pump leakage is the cause for the reduced volumetric efficiency.

There is a rapid reduction in flow as outlet pressure is initially increased. At higher pressures, the rapid reduction subsides and is followed by a flow rate gradient of predicted magnitude. The high pressure gradient can be explained by leakage, but it is difficult to reason that the initial flow reduction is due to leakage because of the low pressure differential range in which it occurs. To verify this conclusion experimentally, the thrust bearing clearances were increased so as to increase the leakage rate of the pump. Further operation at 14,500 rpm produced similar results, with the only change being an increase in the slope of the high-pressure section of the curve The initial flow reduction remained unchanged.

In an effort to determine the cause of the initial flow reduction, a series of experiments was performed. The effect of changes in centrifugal charging pressure was determined by using a larger diameter impeller, which increased the pressure 65 to 70 percent. The outlet pressure corresponding to zero pressure differential across the vane pump stage was increased a like amount. Operation at 14,500 and 25,000 rpm with no change in flow-rate performance indicated that insufficient charging pressure was not the cause.

The vane pump stage was initially designed with approximately 11° of vane sealing overlap in the pumping and sealing lap spaces. The inlet and outlet ports had been so placed that two vanes were on a lap space during the overlap angle of motion. It appeared that the trapped volume between vanes might be expanding during this overlap motion, creating a localized cavitation condition. This could create vane tracking problems and leakage past the vane tips or compressibility type flow losses. The overlap was reduced to 2° by modification of the cam ring ports, but the succeeding tests failed to show any changes in the pump operating characteristics.

To insure that the fuel in the undervane pumping volumes was not cavitating due to undervane port restrictions during the inlet stroke of the vane, the undervane ports were enlarged. The undervane pumping volumes represent 34 percent of the total pump capacity, and compressibility losses due to localized cavitation in these areas would produce a large flow loss. The revision "C" design reflects the modifications necessary to increase the size of the undervane ports. The subsequent evaluation of this modification again failed to indicate any changes in flow rate performance.

The evaluation of the revision "C" parts, however, did produce information which has led to the cause of the flow reduction. During the evaluation, a high-response pressure transducer was used to monitor the outlet pressure. A pressure pulsation at six times rotor rpm was noted for all speeds. The magnitude of this ripple increased as outlet pressure increased, and the revision "C" modifications caused this magnitude to increase rather than decrease. Pulsations as high as 280 psi peak to peak at a frequency of 180,000 cycles per minute were produced when the pump was operated at 30,000 rpm and 420 psig outlet pressure. In addition, wear damage was noted on the underside portion of the stepped vane where the top edge of the floating vane contacted it durings its motion through the pumping lap space. A slight amount of unexplained polishing had been noted with the revision "B" parts; inspection of the revision "C" parts indicated that the modifications had caused acceleration of this wear. The appearance of the parts indicated that the floating vanes were impacting in this area.

The floating vane is required to stroke out with the stepped vane on the inlet port to be in proper position to insure pumping lap space vane stability. If it does not stroke out at this time, it will do so on the pumping lap space due to the pressure differential. This delayed motion of the floating vane would cause a reduction in pump flow rate by drawing fluid from the high-pressure discharge port. The delayed motion produces a condition that is equivalent to reducing the undervane pumping capacity. At a low pressure differential, the floating vane will not stroke completely as it passes through the pumping lap space because the force is insufficient. Only partial flow reduction occurs. As the pressure differential is increased, however, the rate of motion is increased so that the complete stroke occurs within the pumping lap space and so that the maximum flow reduction occurs. This explains the initially rapid reduction in flow as the outlet pressure is increased. Because the floating vane's rate of motion would be dependent on the magnitude of the outlet pressure, it is therefore possible that a delayed motion of this part could also cause a pressure-dependent outlet ripple. The ripple frequency would also be six times rotor rpm due to the use of six vanes. In addition, the delayed motion would produce the impacting situation on the stepped vane that was very evident with the revision "C" parts. The magnification of the wear and ripple amplitude with the revision "C" parts is due to the larger undervane porting and the reduced flow restriction that this porting provides. The reduced restriction allows for faster floating vane motion, which would increase both the ripple amplitude and the level of impact damage. The amount of flow reduction remains unchanged due to the fact that the required floating vane stroke was not modified.

A theoretical analysis indicates that this motion would cause a 15-percent reduction in flow. This added to the 5-percent expected loss on the sealing lap space corresponds well with the experimental loss of 15-25 percent for the various evaluation speeds. The experimental loss is determined by using the high-pressure experimental leakage rate to determine the total pump leakage. The remaining flow loss is then attributed to the improper floating vane motion.

To verify the conclusions drawing from the evaluation of the revision "C" parts, the pump was assembled with a 0.010-inch-thick shim placed in the bottom of each deep rotor slot. The effect of this shim is to take up all clearances allowed to provide reasonable tolerances in the fabrication of the pump parts. The shim minimizes the amount that the floating vane is required to stroke in both lap spaces. It was predicted that the flow rate would increase approximately 100 lb/hr at 25,000 rpm due to the stroke reduction. Operation at 25,000 rpm and 300 psig produced a flow of 830 lb/hr. The same conditions, but without the added shims, produced a flow of 720 lb/hr, or 110 lb/hr less. The flow rate performance curves from this experiment are shown in Figure 10.

In addition to the above experiments, pump evaluation was continued at higher rotational speeds using the revision "B" parts.

The pump was operated successfully at 35,000 and 37,500 rpm with zero pressure differential across the vane pump stage. In each case, the test conditions were maintained for 15 minutes. Diassembly after 37,500 rpm revealed that the carbon vane tips were slightly discolored, but they did not show evidence of wear. There was no evidence that the hydrodynamic film between the vane tip and cam ring was breaking down or that this speed represented an upper limit. Slight contact between the faces of one of the thrust bearings was noted after the 37,500-rpm test. The carbide faces proved to be resistant to galling under these conditions, but the cause of the contact was not established. Previous bearing evaluations at higher speeds had not produced contact, even though the cam ring thrust faces were distorted due to the light press fit during cam ring assembly. This thrust face does not support the centrifugal axial thrust load, but it is possible that the drive system placed an axial load on this bearing due to wear of the keyways and a resulting increase in axial drag. Further evaluation at higher speeds was terminated at this point, however, until the pump endurance capability of 37,500 rpm was verified.

A minor structural failure of two revision "B" stepped vanes occurred during the pump evaluation at 30,000 rpm with an outlet pressure of 470 psig. After 10 minutes at the operating conditions, the 0.012-inch vane wall separating the undervane areas fractured in both vanes.

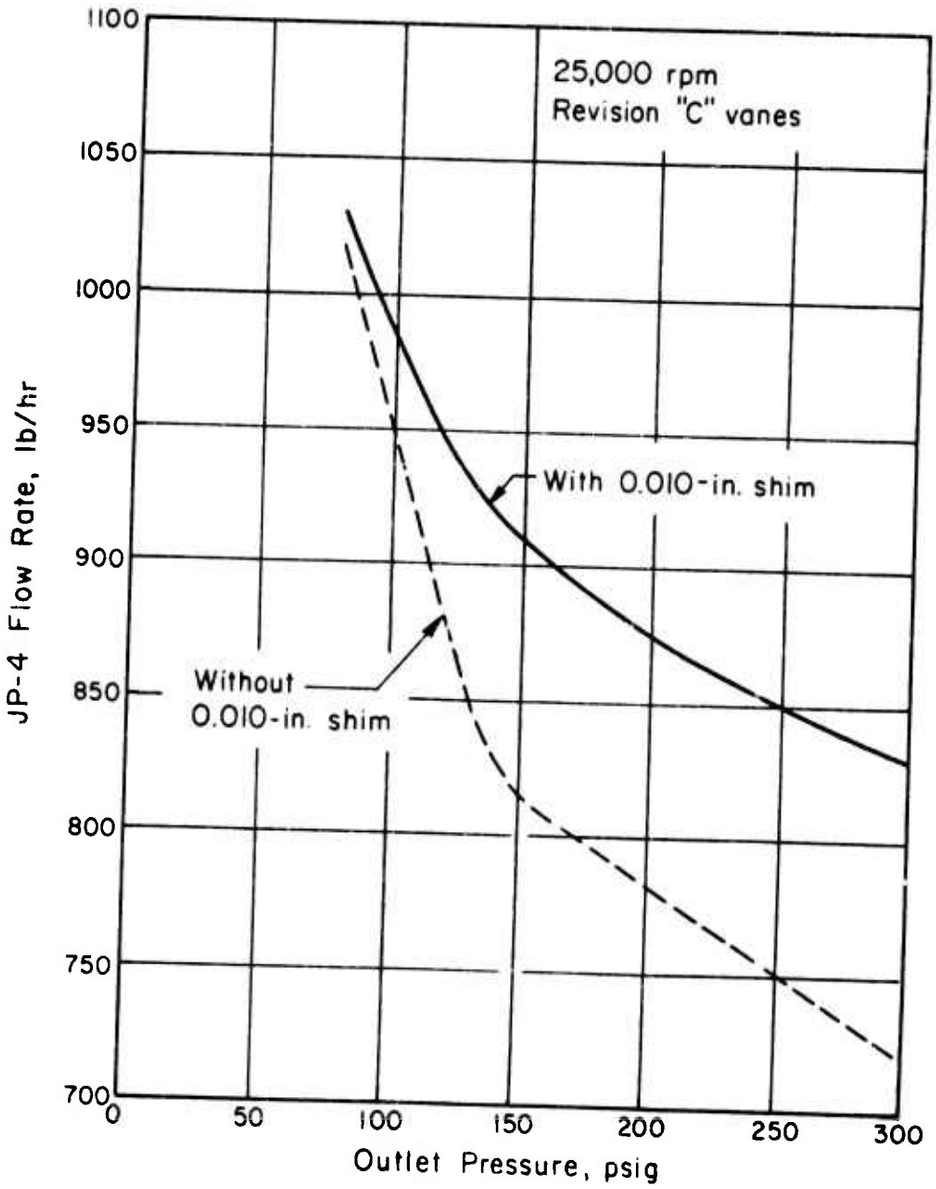

Figure 10. Results of Flow-Reduction Experiment.

One vane tip was cracked by the resultant vane debris, but the failure caused no other damage. During the revision "C" modifications, the stepped vane was strengthened in this area. Subsequent evaluation at higher pressure with the revision "C" parts has been attempted without additional failures.

The impact damage on the stepped vane had occurred at relatively low pressures over a short period of pump operating time. The rate of wear indicated that a premature failure of this part would occur if the pump were operated at the 100 percent speed fuel pressure of 650 psig for extended periods of time. To increase the life capability for further high-pressure and endurance evaluations, a hardened spring steel shim was added to the vane assembly as shown in Figure 11. The 0.0105-inch-thick shim provides a more impact-resistant surface for the floating vane to impact against. The revision "C" vanes were modified slightly so that the required sealing lap space clearances could be maintained with the addition of the shim. This configuration has been successfully operated at 30,000 rpm with an outlet pressure of 600 psig. The complete flow performance curve is shown in Figure 12 and includes the 180,000-cycle-per-minute ripple magnitudes for various outlet pressures up to 600 psig. It is the configuration in Figure 11 that was used during the endurance evaluation.

Several experiments were performed in an attempt to determine the cause of and to eliminate the delayed motion of the floating vane. It has been determined that proper floating vane motion occurs when the vane pump stage is motoring at very low outlet pressures. Under those conditions, the pump flow rate is greater than the theoretical capacity due to floating vane action. The increased flow is due to a portion of the undervane capacity participating twice per revolution in the pumping action. To obtain the increased flow, the floating vane is required to stroke completely in the inlet port prior to being subjected to a pressure differential at the pumping lap space.

Proper floating vane motion was also produced in an experiment which simulated reverse rotation of the vane pump stage. By reversing the rotor axially and driving it from the end to which the centrifugal stage is normally attached, the leading and trailing edges of the vanes are reversed. This operational mode would produce theoretical flow if the floating vane is delayed during the inlet port phase of one revolution. If the floating vane strokes in the inlet port, however, a significant reduction in flow would occur due to a reverse stroking of the floating vane on the pumping lap space. This reduction in flow was the reason for the rejection of this type of design during the revision "B" modification studies. Operation of the pump, assembled as described, at 15,000 rpm produced a very significant reduction in flow as outlet pressure was increased

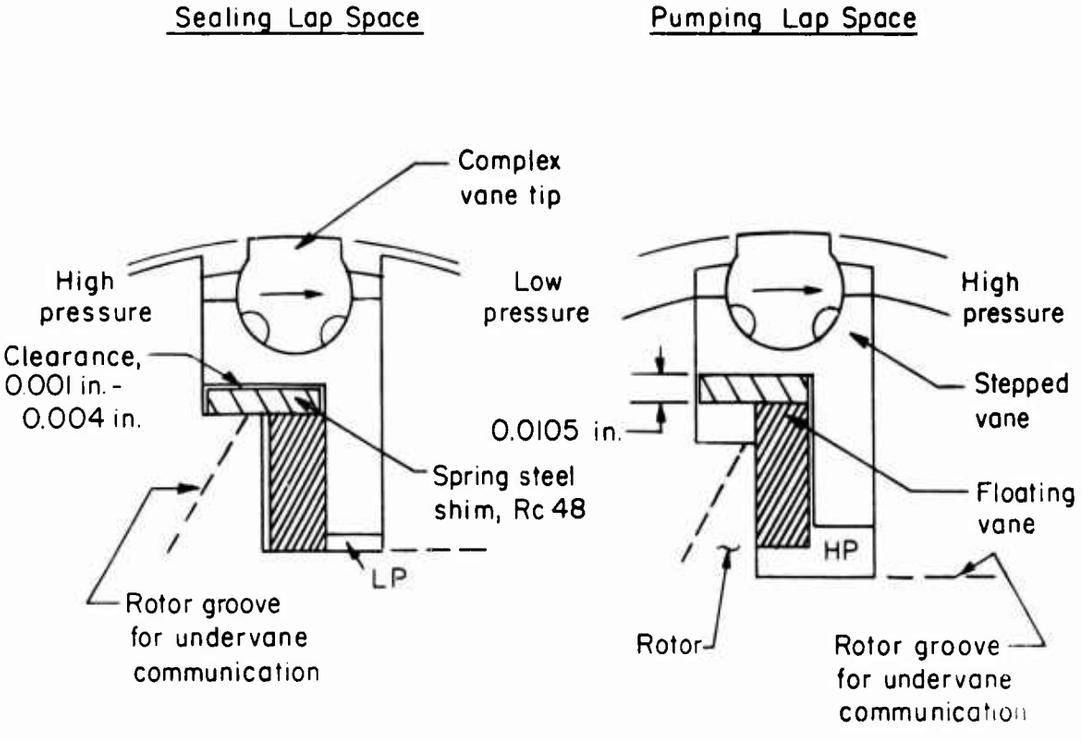

Figure 11. Vane Modification To Improve Impact Resistance.

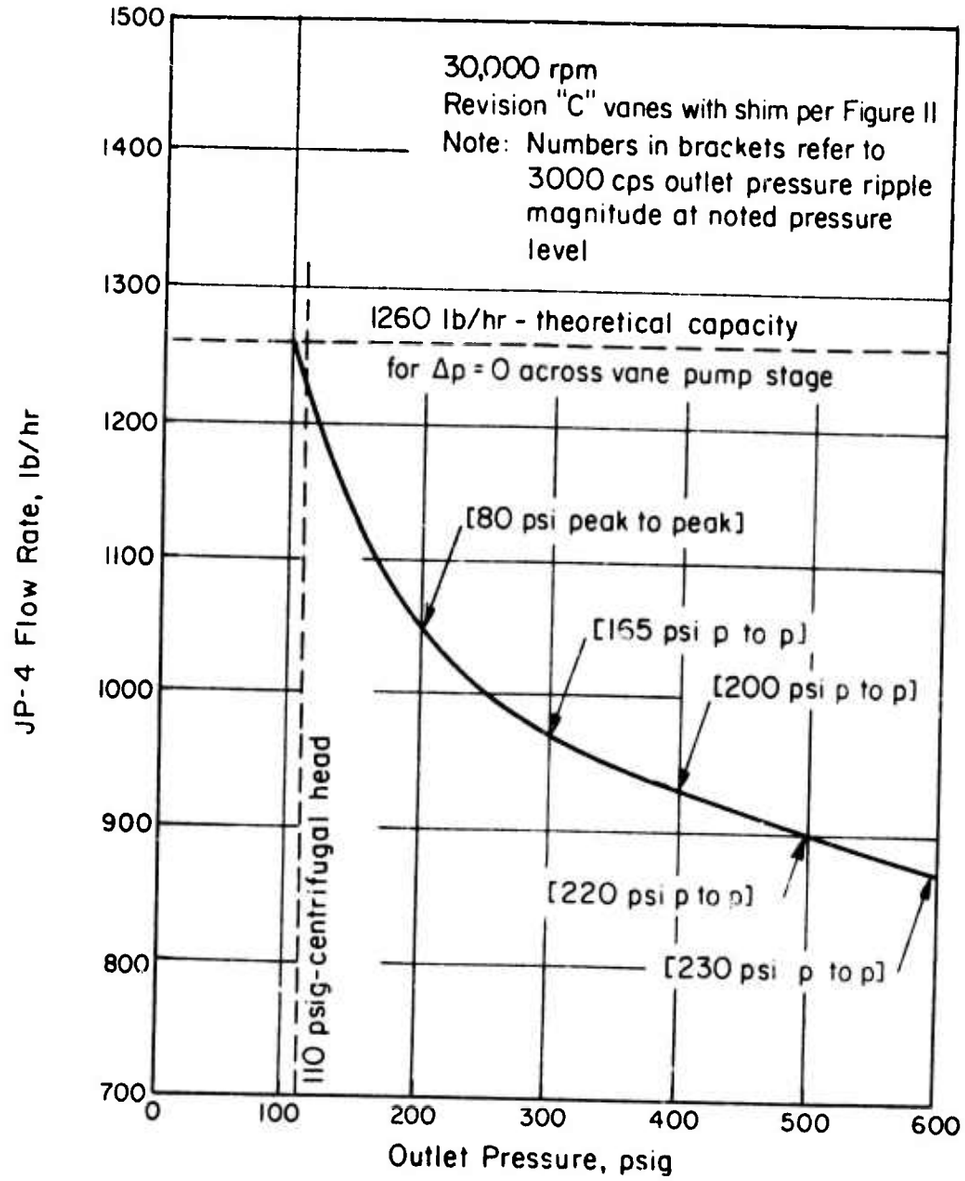

Figure 12. Experimental Flow-Rate Performance, Revision "C" Fuel-Pump Configuration.

above the charging pressure. The results indicated that the floating vane was stroking completely on the inlet port under these conditions and not being delayed as earlier pumping configurations had shown.

The magnitude and the nature of the retarding forces which delay the floating vane motion on the inlet port have not been determined. Floating vanes fabricated from steel in an effort to increase their centrifugal force and to overcome the retarding forces also proved to be inadequate. A crude modification to the steel floating vanes and the revision "B" stepped vanes which allowed the floating vane to be pulled out by the stepped vane as the stepped vane stroked on the inlet port was partially successful in reducing the amount of flow reduction. This experiment verified earlier results, but the parts were of inadequate structural strength to be used for further pump evaluation. Their dimensional accuracy was also insufficient to completely eliminate the flow reduction. Some additional concepts have been developed that attack this problem without compromising the advantages of the two-piece vane configuration. One of these is shown in Figure 13. Further hardware evaluations were terminated, however, due to insufficient time and funding.

It should be noted at this point that the pump is completely operational in spite of the delayed motion of the floating vane. The resultant flow reduction and outlet pressure ripple conditions will require additional study, but preliminary endurance and speed capability limits have been established for the basic pump concept. The impact wear on the stepped vane is sufficiently reduced by the additional steel shim to allow present pump hardware to perform without having its life severely reduced.

The overall pump efficiency is lower than the original theoretical predictions. Figure 14 gives this efficiency and the input power for several operating points at speeds up to 30,000 rpm. In addition, the input power for pump operation with zero pressure differential across the vane pump stage is given for speeds up to 37,500 rpm to indicate the total power allocated to the centrifugal stage, the bearings, the vane tip and rotor drag, and the flow losses. Table IV itemizes the individual experimental losses for the 30,000-rpm, 600-psig test condition results shown previously in Figure 12.

The low overall pump efficiency is due to two factors: (1) very low centrifugal stage efficiency (approximately 11%) and (2) the low vane pump volumetric efficiency. At the 30,000-rpm, 600-psig test conditions, 44% of the input power was required to drive the centrifugal stage. The 110-psig centrifugal head developed at this speed is approximately 2.5 to 3 times that required to theoretically charge

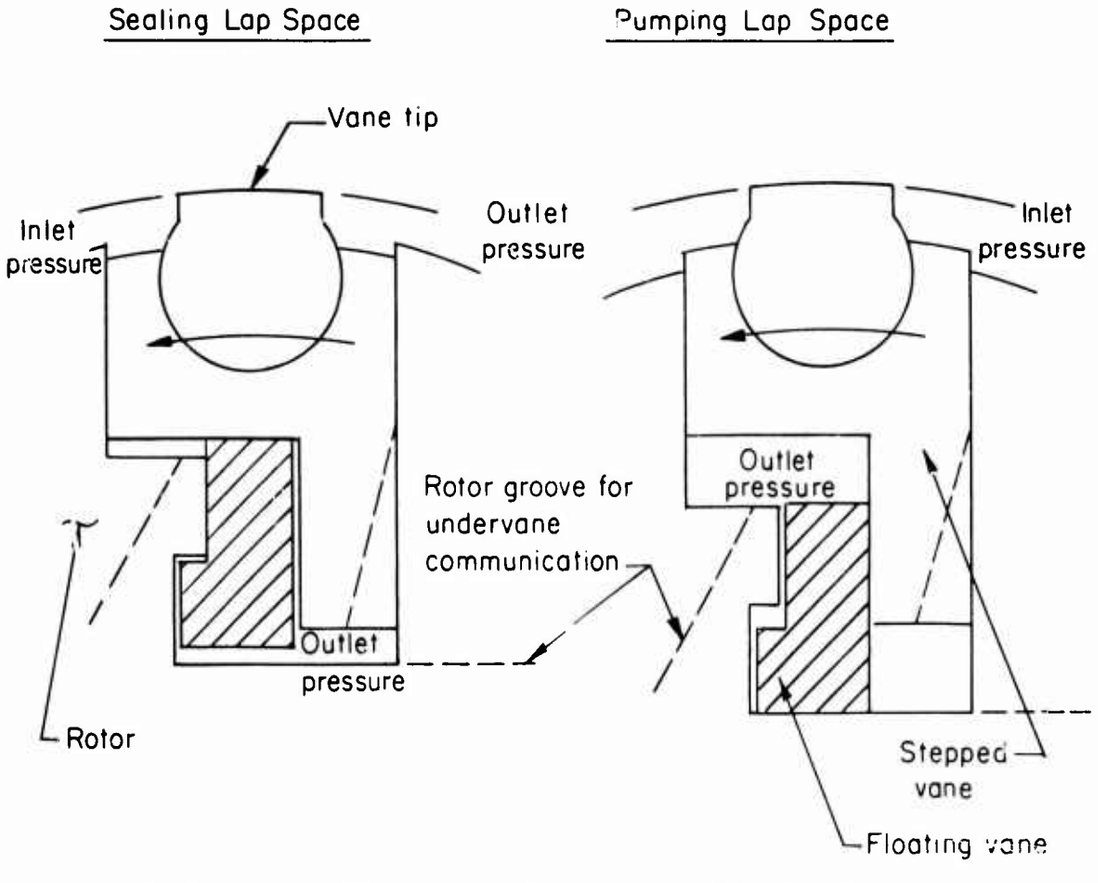

Note: 1. Floating vane performs sealing function between undervane areas when subjected to a differential pressure.

2. Floating vane not required to stroke with stepped vane on inlet port. Step in floating vane and rotor slot insures that total motion is minimized. Flow losses due to floating vane motion are reduced.

Figure 13. Proposed Vane-Assembly Configuration.

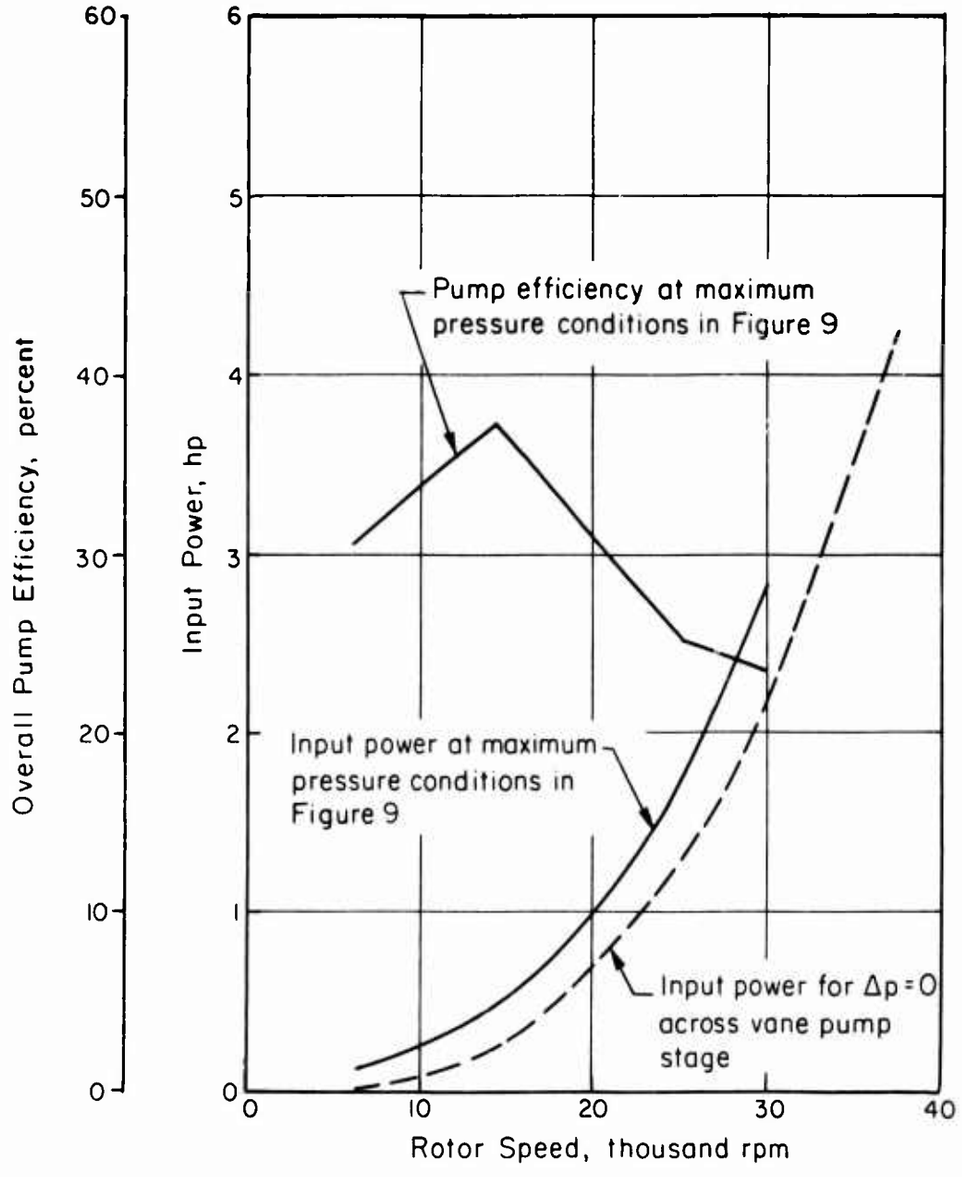

Figure 14. Experimental Input Power and Overall Efficiency.

the vane pump stage. This level of charging pressure provides an ample safety margin for low inlet pressure operation and also reduces pump efficiency at high speeds, where a larger percentage of the developed head is produced by the centrifugal stage. A better flow match between stages and a more efficient diffuser section would reduce the power required by the centrifugal stage. A 30%,centrifugal stage efficiency would increase the overall pump efficiency to 37% at 30,000 rpm, 600 psig. Higher centrifugal stage efficiencies above 30% would probably be difficult to obtain, considering the low specific speed requirements of this application. Improvements in the undervane flow participation, however, could easily raise the volumetric efficiency to 80%. This would increase the overall efficiency to 42%, with a 30% efficiency centrifugal stage producing the present head at 30,000 rpm. A decrease in the developed centrifugal head would also help, but experimental verification of total pump operation at low inlet pressure and high vapor/liquid ratio would be required to determine how much this decrease would be.

TABLE IV. DISTRIBUTION OF INPUT POWER AT 30,000 RPM, 600 PSIG, AND 870 LB/HR

Description	Power Consumption (hp)	% of Total Input
Bearing & rotor drag plus flow losses	0.67	22
Centrifugal stage (Centrifugal flow requirement is 870 lb/hr + 155 lb/hr leakage or 1025 lb/hr)	1.33	44
Theoretical hydraulic power developed by vane pump stage (1260 lb/hr at a 490-psig pressure differential)	0.95	31.5
Vane tip drag	0.08	2.5
Total input power (Sum of above experimental values)	3.03 hp	
Total input power as measured during complete pump evaluation	2.99 hp	
Hydraulic output power	0.81 hp	
Pump overall efficiency		27
Pump volumetric efficiency		69

The viscous drag due to the bearings is higher than the theoretical predictions, but major reductions in the power consumed by the bearings seems improbable due to the high rotational speeds and the close clearances required for proper load capability. The vane tip drag, however, is very low, and the resulting mechanical efficiency of the vane pump stage is high.

Based on the above pump evaluation data, it appears that an overall efficiency of approximately 50% at 30,000 rpm, 600 psig represents a realistic maximum. At lower speeds, where the bearing and centrifugal losses are reduced considerably, the overall efficiency should increase in spite of the lower volumetric efficiency. With increasing speed, however, the centrifugal and bearing losses will become a larger percentage of the required input power.

The temperature rise across the pump for various operating conditions is shown in Table V. The temperatures were measured at the pump inlet and after the outlet pressure was reduced to inlet pressure by dropping it across the pump discharge valve. The rise is also given for operation without the vane and vane tip assembly, to indicate the contribution of the bearings and the centrifugal stage.

TABLE V. FUEL-TEMPERATURE RISE

RPM	Test Conditions	Temperature Rise (°F)
6,000	Centrifugal + bearings; 4 psig, 115 lb/hr	4
	Complete pump; 195 psig, 115 lb/hr	7
14,500	Centrifugal + bearing; 30 psig, 395 lb/hr	5
	Complete pump; 300 psig, 396 lb/hr	8
25,000	Centrifugal + bearings; 80 psig, 710 lb/hr	11
	Complete pump; 400 psig, 710 lb/hr	13
30,000	Centrifugal + bearings; 110 psig, 870 lb/hr	13
	Complete pump; 600 psig, 870 lb/hr	19
37,500	Complete pump; 160 psig, 1550 lb/hr	15

After completion of the 200-hour endurance run and the contaminated fuel evaluation, the experimental fuel-pump performance was evaluated when operating at a higher fuel inlet temperature and at a reduced inlet pressure. These evaluations were of short duration and the objective was to determine whether the pump design had any basic limitations when operating under the more severe environmental conditions.

The pump was successfully operated at 25,000 rpm with a 7.6-psia inlet pressure and a 100-psig outlet pressure. The fuel inlet temperature was 51°F. A Plexiglas centrifugal stage housing was used so that the flow through the centrifugal stage to the vane pump stage could be visually observed. The centrifugal discharge pressure was also monitored to determine the effect on its magnitude and to insure that sufficient pressure was applied to the vane pump stage inlet. With atmospheric pressure applied to the pump inlet, the centrifugal discharge pressure was 80 psig and the pump flow rate was 910 lb/hr. When the inlet pressure was reduced to 7.6 psia, the centrifugal discharge pressure decreased to 70 psig, and the pump flow decreased slightly to 900 lb/hr. The flow through the axial inducer visually appeared to have a high level of fuel vapor or air entrained in it. A stable cavitation ring was formed at the centrifugal impeller ID, but the centrifugal discharge flow was free of entrained vapor. The 7.6-psia inlet pressure is approximately 6 psi above the true vapor pressure of the fuel at this fuel temperature. The operating time was only a few minutes, because of the difficulty in maintaining a stable inlet pressure with the present experimental equipment. Further reduction in the inlet pressure was also not attempted because of this difficulty.

The pump was successfully operated at 30,000 rpm with a fuel inlet temperature of 128°F, an outlet pressure of 152 psig, and an atmospheric inlet pressure. The fuel outlet temperature under these conditions was 139°F. The increased fuel temperature was obtained by removing all coolant flow from the fuel heat exchangers. Coolant flow was removed when the fuel inlet emperature was 50°F, and 35 minutes of continuous operation were equired to reach the test conditions. The pump flow rate decreased from 1090 lb/hr to 1050 lb/hr due to the increased leakage with the heated fuel. A 4.5-percent decrease in input power was also noted. The 78°F increase in fuel inlet temperature represents a change from 1.15 centistokes to 0.59 centistokes in the kinematic viscosity of the JP-4 turbine fuel at the inlet to the pump. Further operation at higher temperatures was terminated due to a high level of fuel vapor that was formed at the unsealed outboard pump bearing. This presented a safety hazard in the laboratory.

To determine the effects of the above evaluations on pump performance, the initial 50°F, atmospheric inlet-pressure conditions were repeated. The results definitely indicated that these evaluations did not cause pump performance degradation. A subsequent inspection of the pump components revealed no changes in their dimensions or visual appearance. The pivoting vane tips performed without wear even though the fuel viscosity was reduced. At no time during the above evaluations did the performance data indicate that the pump was operating under marginal conditions. All pump output data were stable.

Endurance Evaluation

The experimental pump has successfully completed a 200-hour endurance run using filtered JP-4 turbine fuel. The operating conditions, the duration at each condition, and the general results and comments are tabulated in Table VI and Figure 15. The basic objective of this evaluation was to establish the life capabilities of the pivoting vane tip. The outlet pressure was maintained at levels low enough to insure that the floating vane impact damage was not excessive. After the life capability of the pump was established in the 24,000- to 30,000-rpm range, the operating speed was progressively increased until 40,000 rpm was reached. Further evaluation at higher speeds was terminated because of bearing wear in the speed increaser drive system. The endurance run was then continued at 30,000 and 35,000 rpm until 200 hours were logged. At no time during the endurance run was there any indication that the maximum speed limit of the fuel pump had been reached. It appears that the 50,000-rpm goal may still be practical with the present design. It should be noted that 200 hours were completed without replacement of the pivoting vane tips or the cam ring. There was also no evidence to indicate that further operation would require that they be replaced. In addition, the bearings and the centrifugal stage are the same parts that have been used for the entire experimental evaluation of the fuel pump.

During the endurance run, the outlet pressure, outlet pressure ripple, input power, fuel flow rate, rpm, and temperature rise across the fuel pump were continuously monitored and recorded at 15-minute intervals. The pump was periodically disassembled for inspection of wear. At each disassembly, the critical dimensions on the vane tips, stepped vanes, and floating vanes were physically measured. All other parts were visually inspected to insure that they were performing properly.

The successful completion of the endurance run has verified the confidence that has been placed in the hydrodynamic pivoting vane tip concept for achieving high surface speeds in a vane pump. Both the physical and visual inspections made on the vane tips during the endurance run gave no indication of wear on the tip bearing pad surface. The results were achieved in spite of the inferior lubricating qualities of the low-viscosity JP-4 turbine fuel. Traces of the pad crown surface made at intervals during the endurance run are shown in Figure 16. These traces show the pad profile in the direction of tip motion and were produced by a "Talysurf" surface analyzer, which allows the surface to be analyzed at 1000X magnification and reproduces the surface profile with an accuracy of $\pm$ 20 μin. Three vane tips monitored during the endurance run had a

30-μin. maximum variation in the pad profile when measured using the above technique. The localized ripple shown in the traces in Figure 16 are due to the porosity of the carbon tip material and were found in the tips after fabrication.

In addition, the inspection of the cam ring surface produced no evidence of hydrodynamic film breakdown. Areas that had shown slight run-in contact during the preliminary pump evaluations with beryllium oxide tips remained unchanged. The minor transition irregularities between cam ring profile radii were the only areas to show any evidence of polishing. This condition was noted at speeds higher than 35,000 rpm. These irregularities were found to be in the 30-μin. range after fabrication, and at higher speeds it is possible that localized contact occurs as the tip bearing pad crosses the transisions. Further fabrication refinements could help to eliminate irregularities, but the results indicate that this is not necessary at speeds up to 40,000 rpm.

Some light scratches in the direction of tip motion were found on the tip bearing surfaces throughout the pump evaluation and the later endurance runs. These were found to have a maximum width of .003 inch and a maximum depth of 200 μin. It is believed that these were caused by particles of the hard anodic coating that were chipping off the sharp edges of the floating vanes. Some additional particles were found embedded in the soft aluminum stepped vanes. The pump digests this level of contamination, however, without affecting hydraulic or mechanical performance.

The trailing edge of the aluminum stepped vane, which had shown some initial run-in wear during the 30 hours of pump evaluation, did not continue to wear appreciably during the endurance run until 35,000 rpm was exceeded. The maximum metal removal after 135 hours at a maximum speed of 35,000 rpm was 0.0003 inch. At higher speeds, two vanes exhibited increased wear and were replaced when this wear exceeded 0.003 inch. The increased wear appeared to be associated with the amount of vane tilt possible in the rotor slot; the rate of wear also increased when the outlet pressure was increased. The leading edge of the stepped vane did not show measurable wear at any time during the endurance run.

As noted above, the hard anodized floating vanes exhibited chipping of the hard anodic coating. During the 32,500-rpm, 25-hour portion of the endurance run, this chipping increased because a 400-psig outlet pressure was maintained. In addition, two of the floating vanes failed and broke into several pieces. This failure was probably caused by the higher impact loading during higher pressure operation.

TABLE VI. ENDURANCE SCHEDULE

Period	Operating Conditions	Results and Comments*
0-50 hr	30,000 rpm; 200 psig (outlet pressures to 350 psig were maintained for 6-1/2 hr)	No indication of pump distress or excessive wear. No parts replaced.
50-100 hr	24,000 rpm; 250 psig	No indication of pump distress or excessive wear. No parts replaced.
100-114 hr	32,500 rpm; 400 psig	Failure of one floating vane. Stepped vane damaged by failure - replaced with spare. Steel floating vane used for replacement. No damage to pump otherwise.
114-125 hr	32,500 rpm; 300 psig	2nd failure of a floating vane. All floating vanes replaced with aluminum floating vanes without the hard anodic coating. The original, hard anodized, floating vanes show considerable chipping of the hard anodic coating.
125-135 hr	35,000 rpm; 200 psig (pressure reduced to minimize floating vane impact damage)	No indication of pump distress or excessive wear.
135-145 hr	37,500 rpm; 230 psig	Stable operating conditions. Flow rate shows no degradation to date. Trailing edge of two stepped vanes shows first sign of increased wear. 0.002 in. maximum metal removal. Other vanes appear unchanged.

* No replacement of pump parts was made except as noted in this column. The same pivoting vane tips and cam ring were used for the entire 200-hr endurance run. These same parts were also used in the contaminated fuel experiment performed after 175 hours of the endurance run.

TABLE VI - continued

Period	Operating Conditions	Results and Comments
145 to 145-1/4 hr	40,000 rpm; 256 psig (first time the pump has operated at this speed)	Trailing edge wear on stepped vanes increasing. Outlet pressure ripple frequency increased to 12X rotor rpm. No indication of vane tip wear. Tips still appear to be maintaining a hydrodynamic film. Attempts to increase speed terminated at this point due to bearing wear in the speed increaser system.
145-1/4 to 155-1/4 hr	35,000 rpm; 200 psig	Continuing stepped vane wear. Sides of aluminum floating vanes show increasing wear now that surface is not hard anodized.
155-1/4 to 156 hr	35,000 rpm; 350 psig (these conditions used to establish effect of high pressure on durability of aluminum parts)	Metal removal on trailing edge of one stepped vane has increased to 0.003 in. Vane replaced with spare. Impact damage due to high pressure not excessive; therefore, pump will be periodically cycled at higher pressure levels.
156-166 hr	35,000 rpm, 200 psig (outlet pressure increased to 350 psig eight times for 15-minute period - total time: 2 hr)	Replaced 2nd stepped vane due to wear on trailing edge. Vane tips in excellent condition.
166-175 hr	30,000 rpm, 150 psig (outlet pressure increased to 250 psig four times for 10-minute period - total time: 40 min)	Speed decreased due to increasing speed increaser wear. Pump performance stable. No degradation of flow rate. Input power steady.

TABLE VI - continued

Period	Operating Conditions	Results and Comments
Contaminated Fuel Evaluation - See Table VII.		
175-176 hr	25,000 rpm, 110 psig to 35,000 rpm, 200 psig (these conditions used to verify the pump's previous high speed capability after the contaminated experiments)	No indication of pump distress or wear. Stable pump performance. Flow rate identical to results obtained prior to contamination experiments.
176-200 hr	30,000 rpm, 150 psig	No indication of pump distress or wear. Slight decrease in input power. No indication of vane tip wear. Tips still appear to be maintaining a hydrodynamic film.

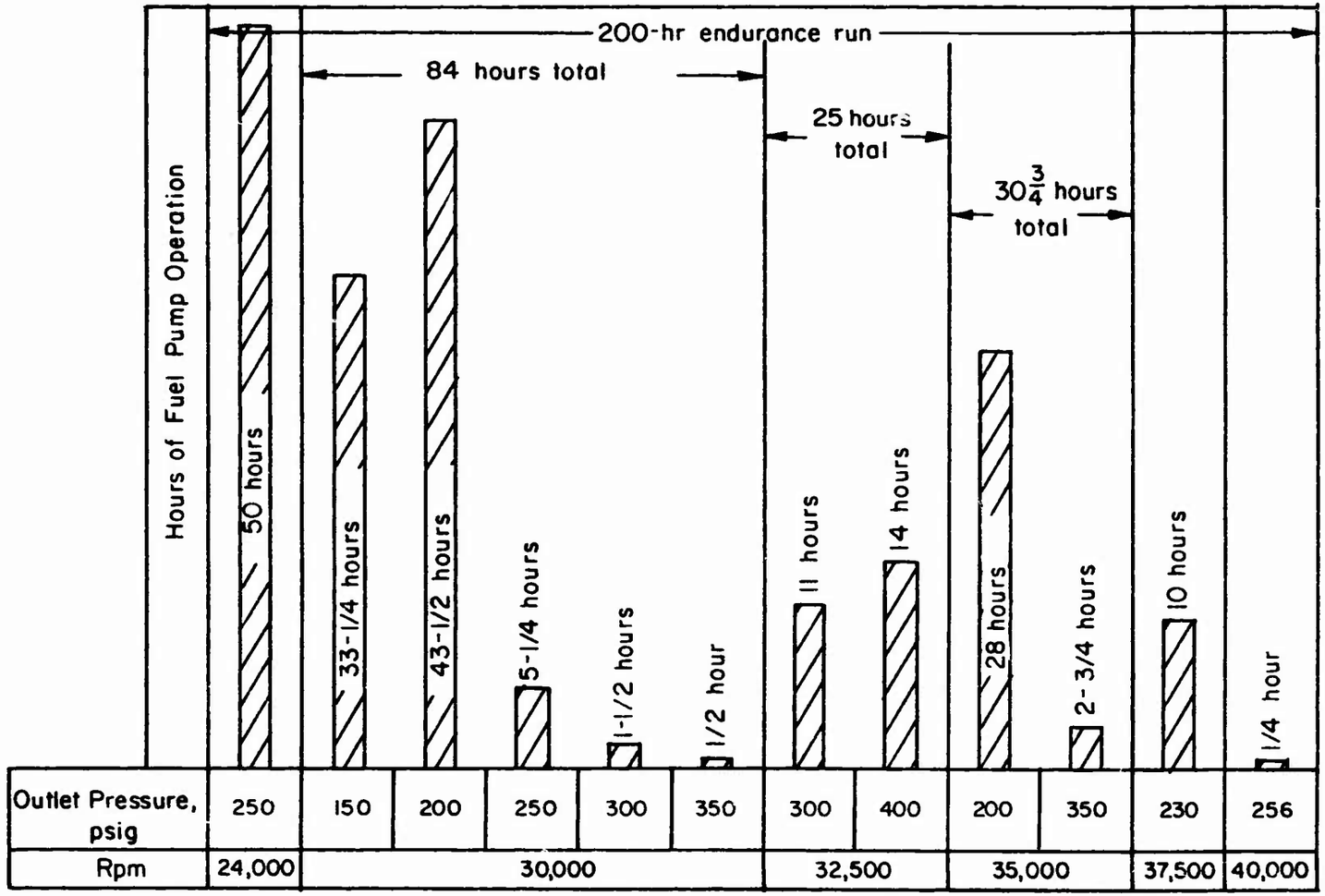

Figure 15. Summary of Pump Endurance Evaluation Conditions.

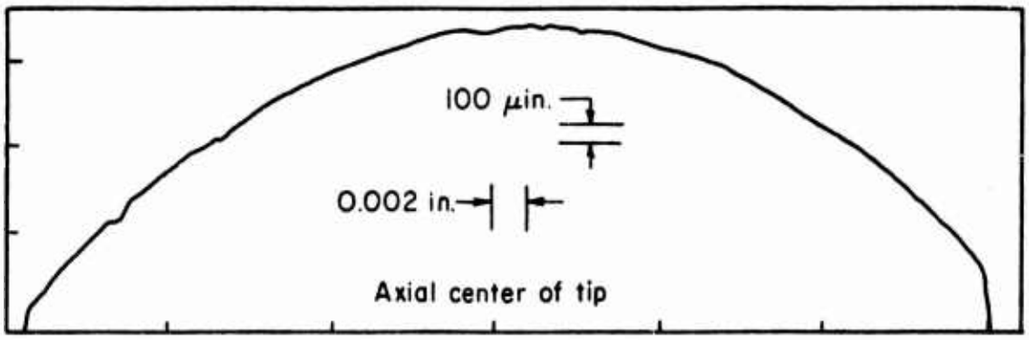

Vane tip pad profile - as fabricated

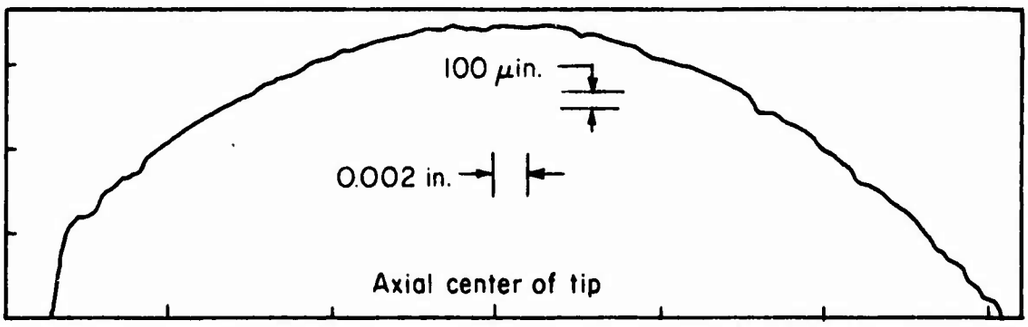

Vane tip pad profile - after 50 hr at 30,000 rpm

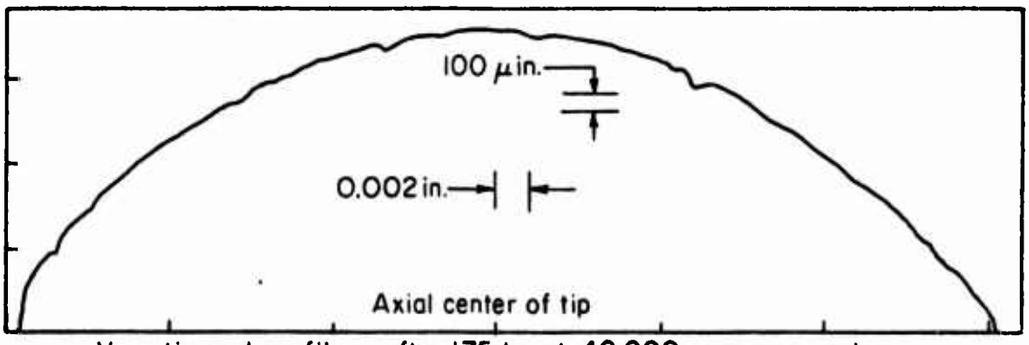

Vane tip pad profile - after 175 hr at 40,000 rpm max, prior to contamination schedule

Figure 16. Vane Tip Inspection Results.

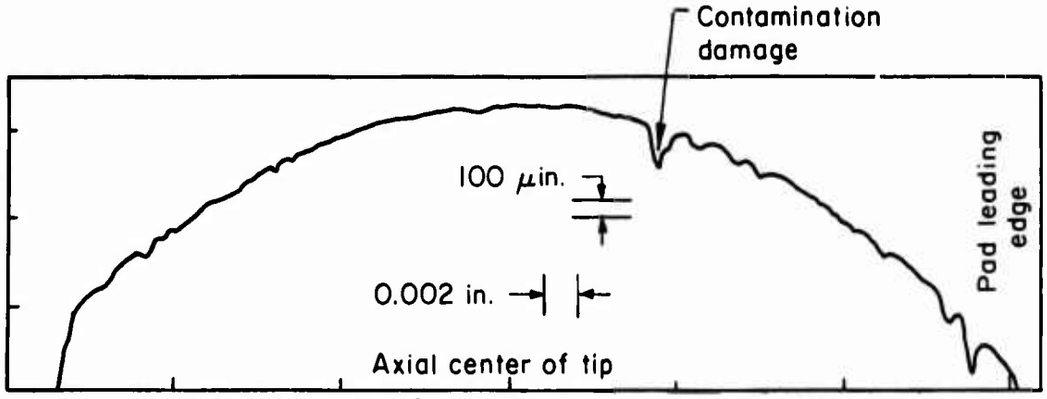

Vane-tip pad profile - after contamination schedule

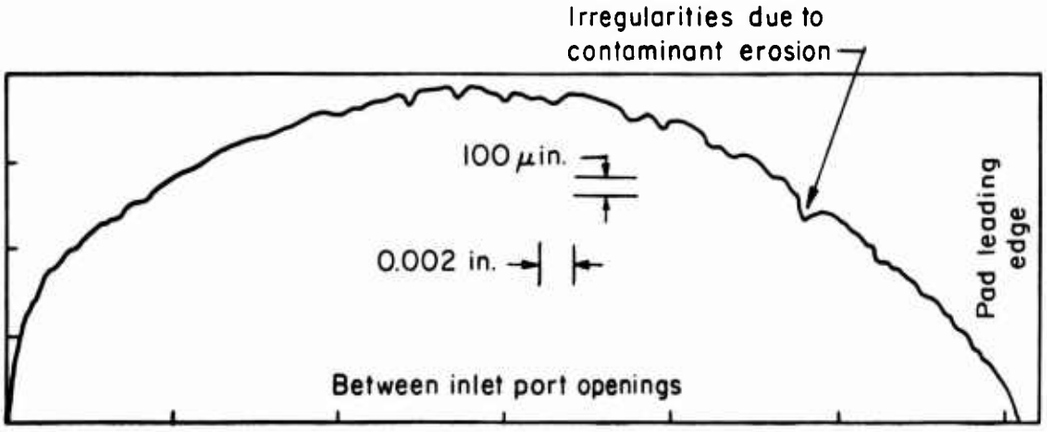

Vane tip pad profile - after contamination schedule,
worst-case condition

Figure 16. Continued

This failure was not noted, however, until the pump was disassembled. Performance was maintained nevertheless, but one stepped vane had to be replaced because of increased undervane wear. The original hard anodized floating vanes were completely replaced with aluminum floating vanes without the hard anodized surfaces. After this, the outlet pressure was not maintained at higher levels for long durations so that the impact damage could be minimized. All further high-pressure operation was done on a cycling basis.

The fuel pump bearings and centrifugal stage performed well during the entire endurance run. They gave no evidence of marginal operation. The high-speed thrust bearing contact noted during the evaluation stage did not increase or cause any problems. Measurement of the journal bearing clearances indicated that the clearances had increased a maximum of 0.0002-inch from the as-fabricated clearances of 0.0008 inch. This includes the damage that occurred during the beryllium oxide tip failures. The abrasive ceramic particles did open up the clearances slightly at that time.

Contamination Evaluation

After completing 175 hours of the endurance evaluation, the pump was subjected to a short contamination evaluation. The objective was to determine if the pump concepts were unduly sensitive to contaminated fuel (MIL-E-5007-C). The endurance capability using contaminated fuel was not evaluated. Some endurance predictions can be made, however, based upon the results of the short contamination runs. Given amounts of contaminant were injected into the pump inlet on a single-pass basis. The contaminated fuel was not continuously circulated from the pump outlet back to the inlet, but it was filtered as it left the outlet of the pump. This was consistent with the objective. It was important to determine if the maximum required contaminant size (420 microns) could pass through the vane pump stage without causing major structural damage to the hydrodynamic vane tips.

Table VII gives a tabulation of the four contamination runs. The pump was disassembled after each run for inspection and thoroughly cleaned prior to the next evaluation. The contaminant was separated into the particle size categories as noted in Table VII so that the effects of a given size could be independently determined.

The contaminant was injected into the pump at 15,000 rpm. The speed was then increased to 25,000 rpm and held to insure that all of the contaminant was removed from the contaminant chamber at the inlet to the pump. The increased flow at 25,000 rpm was sufficient to cause removal of all the contaminant.

The results of the contamination evaluation are very encouraging. Silica sand particles as large as 420 microns (.0165 in.) were accepted by the pump without producing any structural failures. In fact, the larger silica sand particles (177-420 microns) did not appear to have any effect on the pump performance or to cause any abrasive type wear on the pump components. The fine grade of Arizona road dust (A.C. Spark Plug Co. Part No. 1543094), which had particle sizes ranging from 0-80 microns, produced the most wear damage to the pump components. After these fine particles were placed in the pump, approximately a 7% increase in input power was noted. The succeeding runs with larger particles did not produce any further changes in the input power, however. The increase in input power was the only performance deviation noted. The flow rate was stable both during and after the contamination runs and did not deviate from previous results obtained during the endurance evaluation.

Contamination produced visible damage to the aluminum stepped vanes and floating vanes. Some areas on these parts had a sand-blasted appearance, and there was no indication that they had the required endurance capability. The surface roughness of the tip bearing pad surface increased from a 20 μin. to a 40 μin. center line average. The pad surface appeared roughened after the fine dust was used, but this roughness did not increase with succeeding runs. The carbon tip material appeared to have marginal contamination resistance in the area of the bearing pad when subjected to fine, abrasive particles. The tip socket area showed very little indication of damage, however. This was also true of the aluminum vane socket. The contaminant could not penetrate the small clearances in large enough quantity to cause damage. At no time did the inspection after the pump was disassembled reveal any evidence that either the vanes or the tips were not free to move properly. After the fine dust evaluation, there was definite evidence of residual contaminant in the pump and indication of tip and vane drag in their respective motions. The amount of residual contaminant and the vane and tip drag diminished as the particle size increased. After the last silica sand run (250-420 micron), there was no indication of any drag and the results were the same as a run on clean fuel.

Figure 16 shows traces of the tip bearing pad crown after the contamination schedule was performed. The overall configuration remained unchanged on the pads, but considerable erosion was noted in some localized areas. It is important that this configuration remains unchanged so that the tip hydrodynamic bearing capability is not degraded. The erosion noted should not severely affect the load capability, but it would probably cause the tip to run at a smaller film thickness. The smaller film thickness is a likely explanation for the increased input power.

The remaining pump components were only slightly affected by the contamination schedule. The "Ferro Tic C" cam ring and combination journal and thrust bearings did not change in appearance. The bronze sleeves did not show any evidence of wear. Light polish zones found during a previous inspection of these parts remained unchanged and indicated that very little of the contaminant reached the journal bearing area. The results indicate that most of the contaminant remains in the main flow paths in the pump and is ejected through the outlet port. The centrifugal impeller and axial inducer were unchanged.

After the contamination schedule was completed, the pump was cleaned and reassembled, and the endurance evaluation continued. Because of problems with the speed increaser system, the maximum speed did not exceed 35,000 rpm. For 1 hour the fuel pump was operated in the 25,000- to 35,000-rpm range to verify its previous capability. The 7% increase in input power was still noted. A disassembly revealed no additional pump wear. The evaluation continued at 30,000 rpm for 24 more hours, bringing the total endurance time to 200 hours. A slight decrease in input power was noted during the last 24 hours, but the input power was still approximately 4 or 5 percent higher than obtained prior to the contamination schedule. The results did not give any indication that further operation would continue this trend, however. The inspection revealed that subjecting the pump to the contamination schedule had not reduced the pump's high-speed capability and that it was still operational. The flow rate was stable and corresponded to the same level obtained prior to the contamination schedule.

CONCLUSIONS

The basic design concepts incorporated in the experimental fuel pump appear very promising. The high-speed capabilities of the pivoting vane tip concept have been clearly demonstrated, with encouraging results. Speeds as high as 40,000 rpm have been experimentally achieved, and the goal of 50,000 rpm still appears to be feasible. The experimental pump has also provided the information necessary to an understanding of the requirements for vane and vane tip stability under the broad range of fuel pump operating speeds and pressures.

To date, the experimental fuel pump as fabricated is not completely capable of meeting all of the realistic requirements of a gas-turbine fuel pump. The flow reduction and outlet pressure ripple conditions will require further design effort before the required high-pressure pump life is obtained. The floating vane impact condition produces accelerated wear in the undervane area when a vane stage differential pressure of 200 psi is exceeded. The 200-hour endurance run indicates,

TABLE VII. CONTAMINATION SCHEDULE

Contaminant	Particle Size (microns)	Quantity* (grams)	Duration After Contamination Injected Into Pump (minutes)
Fine Arizona Road Dust. A.C. Spark Plug Co. Part No. 1543094	0-80	1/2	25
Coarse Arizona Road Dust. A.C. Spark Plug Co. Part No. 1543637	0-200	1/4	12
Sharp Silica Sand	177-250	1/4	13
Sharp Silica Sand	250-420	1/4	10

* These quantities represent particle densities in the fuel that far exceed the requirements of MIL-E-5007C, particularly since the particles were introduced in a single slug of fuel into the fuel pump. The higher level was chosen because the particles were injected on a single-pass basis.

however, that a high-speed, long-life fuel pump is definitely feasible. The total vane tip bearing pad profile change of less than 50 μin. during the endurance run is a significant achievement, considering the high surface speeds.

The overall efficiency of the experimental fuel pump is relatively low, but significant improvements appear to be possible with optimization of the centrifugal stage design and improved vane pump stage volumetric efficiency. The centrifugal stage design proved to be capable of supplying the required charging pressures at all speeds and performed successfully at low inlet pressure conditions. High-speed bearing life and performance have also been obtained using the low-viscosity turbine fuels as a lubricant.

The contaminated fuel experiments have indicated positively that the basic design concepts are not unduly sensitive to contaminated fuel. It is felt, however, that considerable effort will be required in the area of component materials selection to insure that a high-speed fuel pump of the type described will have adequate life under long-term exposure to contaminated fuels.

The use of the basic fuel pump concepts with hydraulic pumps appears to be feasible. It should be pointed out, however, that the speed and pressure limits have not been experimentally established. Presently, it appears that speeds of 30,000 rpm and pressures approaching 3000 psig are realistic, particularly for low-capacity pumps.

The low-outlet-pressure requirements of a lubrication pump make the use of any high-speed positive-displacement pump unattractive for lubrication pump applications.

RECOMMENDATIONS

It is recommended that the high-speed fuel pump development be continued because of the highly encouraging results obtained to date. It is felt that further effort should be applied to the determination of the performance limits for the basic concepts and the development of the high-pressure, endurance capability that has not been demonstrated to date. The following is a list of suggested areas for future research:

1. Development of an undervane pressure distribution system that eliminates the present high-pressure floating vane impact conditions.

2. Determination of the pivoting tip speed limitations. Not only should this consider the present configuration, but it also should attempt to establish more completely the geometric conditions necessary for optimization of the tip performance.

3. Basic materials studies to improve both the endurance and the contamination capabilities of future hardware. The effects on the ease of pump fabrication should also be considered.

4. Investigation of structural improvements that could increase pump performance and simplify pump fabrication.

5. Optimization of the centrifugal stage design to improve overall pump efficiency.

6. Determination of the effects of shock and vibration and the sensitivity of the basic components to these environmental conditions.

In addition, it is suggested that some consideration be given to a variable-displacement fuel pump after the fixed-displacement concepts have been fully established. The basic technology for high-speed operation has been established, but a considerable improvement in the overall fuel system performance could also be gained if a variable-displacement capability could be developed. The development of a variable-displacement fuel pump appears to be feasible, based on the results of the present research. This development would probably evolve directly from the present fixed-displacement vane pump concepts.

LITERATURE CITED

1. Swain, J. C., et al, "Concept and Design Analysis for a Variable-Displacement, 'Turbine-Speed' Hydrostatic Pump", Battelle Memorial Institute; Department of the Army Project No. I-D-543003-D-395, U.S. Army Tank Automotive Center, Warren, Michigan, May 1965, AD 467 877L.

2. Thomas, D. L., Wilcox, J. P., and Mitchell, R. K., "Investigation of a 30,000-rpm Turbine-Speed Hydraulic Pump", Battelle Memorial Institute; Technical Report AFAPL-TR-68-5, U.S. Air Force Aero Propulsion Laboratory, Wright-Patterson Air Force Base, Ohio, June 1968, AD 834 312.

3. Swain, J. C., Thomas, D. L., Slabiak, W., and Santo, H. A., "A Turbine-Speed Pump for Vehicle Transmission Use", SAE Paper No. 670954 for Combined Fuels and Lubricants, Powerplant and Transportation Meetings, October 30 - November 3, 1967.

4. Raimondi, A. A., and Boyd, J., "The Influence of Surface Profile on the Load Capacity of Thrust Bearings with Centrally Pivoted Pads", Trans. ASME, Vol 77, 1955, pp 321-330.

5. Raimondi, A. A., "The Influence of Longitudinal and Transverse Profile on the Load Capacity of Pivoted Pad Bearings", Trans. ASLE, Vol 3, No. 2, 1960, pp 265-276.

6. Nixon, James, et al, "Investigation and Analysis of Aircraft Fuel Emulsions", Esso Research and Engineering Company; USAAVLABS Technical Report 67-62, U.S. Army Aviation Materiel Laboratories, Fort Eustis, Virginia, November 1967, AD 827 051.

7. Harris, J. C., and Steinmetz, E. A., "Investigation and Analysis of Aircraft Fuel Emulsions", Monsanto Research Corporation; USAAVLABS Technical Report 67-70, U.S. Army Aviation Materiel Laboratories, Fort Eustis, Virginia, December 1967, AD 668 248.

SELECTED BIBLIOGRAPHY

Csanady, G. T., Theory of Turbomachines, New York, McGraw-Hill Book Company, 1964, p 378.

Ross, C. C., and Banerian, G., "Some Aspects of High-Suction Specific-Speed Pump Inducers", Trans. ASME, Vol 78, 1956, pp 1715-1721.

Braske, U. M., "Development of Some Unconventional Centrifugal Pumps", Proc. Inst. Mech. Engrs. (London), Vol 174, No. 11, 1960, pp 437-461.

Rippel, Harry C., "Cast Bronze Thrust Bearing Design Manual", Cleveland Cast Bronze Bearing Institute, Inc., May 1967, p 117.

Abramovitz, Stanley, "Theory for a Slider Bearing with a Convex Pad Surface; Side Flow Neglected", Journal of The Franklin Institute, Vol 259, No. 3, March 1955, pp 221-233.

Wildmann, M., et al, "Gas-Lubricated Stepped Thrust Bearing - A Comprehensive Study", ASME Paper No. 64-LubS-6, April 1964, p 17.

Osterle, F., Charnes, A., and Saibel, E., "On the Solution of the Reynolds Equation for Slider-Bearing Lubrication--IV (Effect of Temperature on the Viscosity)", Trans. ASME, Vol 75, 1953, pp 1117-1123.

APPENDIX I
THEORETICAL ANALYSIS OF VANE ASSEMBLY DESIGN

NOMENCLATURE

Parameter	Description	Nominal Value	Units
a	(See Figure 17)	0.030	inches
B	Tip pad width	0.060	inches
b	(See Figure 17)	0.030	inches
C	Load variable	---	dimensionless
d_1	(See Figure 17)	0.012	inches
d_2	(See Figure 17)	0.012	inches
h	Film thickness	---	inches
h_o	Minimum film thickness	---	inches
p	Pressure	---	psig
p_1	Pressure in front of vane	---	psig
p_2	Pressure behind vane	---	psig
U	Velocity of vane tip pad	---	in./sec
W	Load capacity	---	lb/in.
x	(See Figure 17)	---	inches
μ	Viscosity of JP-4 (80°F)	0.84×10^{-7}	$lb\text{-}sec/in.^2$

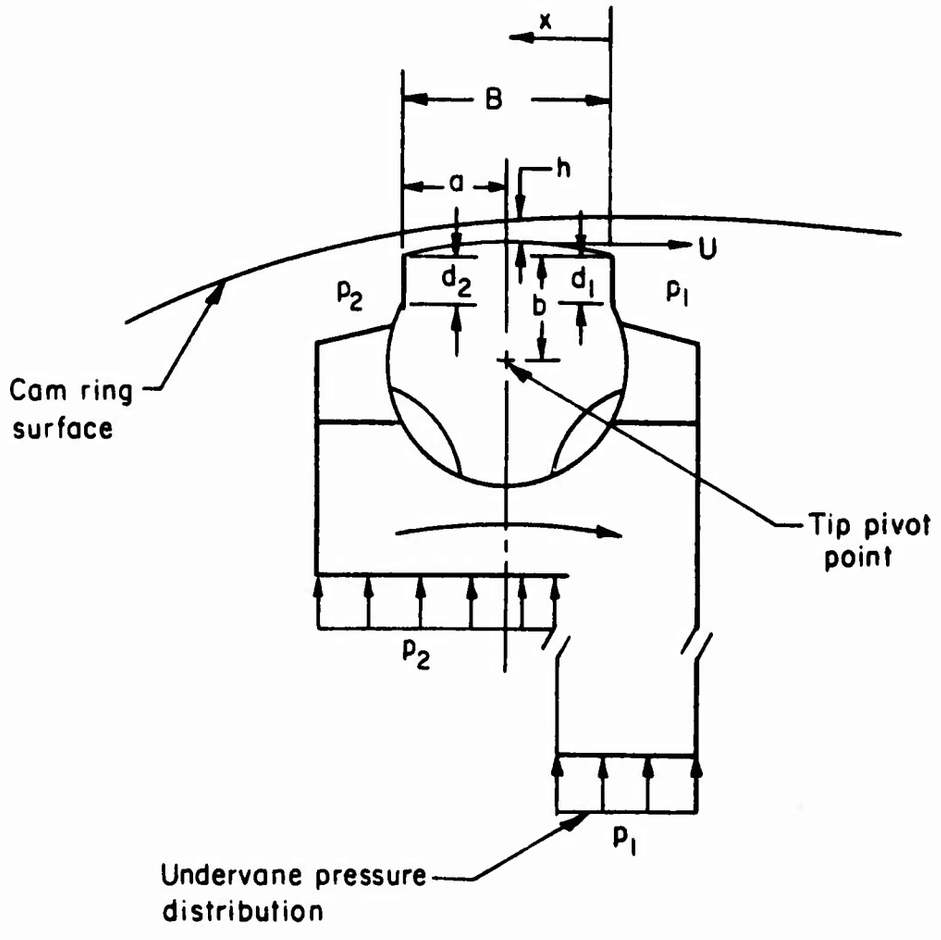

Figure 17. Vane Tip Schematic.

PIVOTING VANE TIP ANALYSIS

The pivoting vane tip operates as a centrally pivoted pad thrust bearing. It is self-acting, and the pressure in the fluid film between the tip bearing pad and the cam ring surface is hydrodynamically generated by the relative motion between the surfaces. The resulting hydrodynamic pressure profile is charged with supporting the centrifugal loading of the vane assembly plus any chosen hydrostatic radial unbalance and the radial drag forces due to inward stroking of the vane.

The factor which is of most significance in contributing to the load capacity of a centrally pivoted pad is the relative surface profile between the pad and the cam ring.[4,5] For this reason, considerable effort was devoted to determining the proper relationship between the tip pad radius and the cam ring radii for various pad widths, B. The results of this analysis played an important part in the final design configuration of the vane pump stage.

A computer program developed by the Battelle Columbus Laboratories to study this problem in previous high-speed vane pump designs was used during this analysis. The program is based upon the solution of the usual Reynolds equation for the no-side-flow condition.

$$\frac{\partial}{\partial x}\left(\frac{h^3}{\mu}\frac{\partial p}{\partial x}\right) = 6U\frac{\partial h}{\partial x} \qquad (1)$$

This two-dimensional analysis neglects bearing side flow along the length, but the long vane tip length in comparison to the pad width makes the assumption reasonable. The additional assumptions involved are that the fluid viscosity is considered constant and that the fluid is incompressible. These assumptions are realized when low-viscosity lubricants such as water are used. Preliminary experiments with JP-4 also indicated good correlation with this theoretical approach.

The resulting load capacity per unit length is given by

$$W = C\frac{\mu UB^2}{h_o^2} \qquad (2)$$

The load variable (C) is a function of the relative surface profiles, the magnitude of the minimum film thickness (h_o), and the position of the point of minimum film thickness as measured from the pad leading edge.

A pivoted pad exposed to a uniform hydrostatic pressure field will automatically rotate to a position of stable equilibrium. Equilibrium occurs when the resultant force produced by the hydrodynamic pressure profile passes through the pad pivot, eliminating all moments applied to the pivoting vane tip. The application of this concept to a vane pump requires that the effects of a hydrostatic pressure differential across the pad width also be investigated to determine the requirements for tip rotational equilibrium under this condition. The computer program is designed to calculate the hydrostatic pressure distribution on the bearing pad and the resulting moment generated for varying tip positions and minimum film thicknesses. This is combined with the results of the hydrodynamic profile analysis to determine if a condition of stable rotational equilibrium exists for the operating conditions required for the fuel pump application.

For a given minimum film thickness, the program calculates the net moment applied to the tip and the load capacity of the tip as the point of minimum film thickness is moved from the leading edge to the trailing edge of the pad in small steps. The program essentially rotates the tip through various positions until a position of stable equilibrium is achieved. The achievement of equilibrium requires that the net moment applied to the tip be zero and that if the tip is rotated slightly from this position, the resulting moment be of proper direction so as to return the tip to the equilibrium position.

A revision "A" tip design (without the raised pad) requires that the moment generated by the hydrostatic pressure differential on either the pumping or the sealing lap spaces be counterbalanced by the self-generated hydrodynamic pressures of the bearing because all other pressures applied to the tip produce forces whose resultants pass through the tip pivot point. When the magnitude of the hydrostatic pressure profile is much larger than that of the hydrodynamic pressure profile, a condition results in which a stable rotational equilibrium point does not exist. The required orientation between the tip bearing pad and the cam ring necessary for noncontacting operation cannot then be maintained. The lower hydrodynamic pressures occur in the fuel pump at the low-speed conditions when the resulting vane assembly centrifugal loading is considerably reduced. The low relative surface speed and large film thickness produce a situation in which the slightly reduced hydrostatic pressures predominate by a large factor. This situation could also occur at higher speeds if large film thicknesses were maintained, but the high centrifugal loading can be supported by the bearing only at relatively low film thicknesses in which the hydrodynamic pressure is large.

To produce stable tip equilibrium at the pump low-speed operating conditions, it is necessary to provide a hydrostatically generated counterbalancing moment. The revision "B" raised-pad design fulfills this requirement. The vertical lands serve to produce counterbalancing

moments which automatically reverse direction in phase with the normally unbalanced bearing pad surface moments. The result is a tip which is stable independent of the pump speed and the outlet pressure magnitude. Figure 18 shows the hydrostatic pressure distributions on a tip of this design for both the pumping and the sealing lap spaces.

VANE RADIAL STABILITY ANALYSIS

The object of the vane design is to produce an undervane pressure distribution which causes the vane assembly to track the pump cam ring profile without lifting off the cam surface and which at the same time does not produce excessive loading between the pad bearing surface and the cam ring. The computer program described previously is designed also to calculate the requirements for balancing the radial forces applied to the vane assembly and therefore provides the tool by which this problem can be analyzed.

The stepped vane and resulting undervane communication technique place the vane assembly in a uniform hydrostatic field during the inlet and outlet port segments of the pumping cycle. Proper tracking in these areas is determined by the cam ring profile design. On the lap spaces, however, the effect of a hydrostatic pressure distribution on the bearing pad produces an inward force on the vane assembly. To insure vane tracking at lower pump speeds and high outlet pressure, it is necessary that this force be balanced by the undervane pressure distribution as shown in Figure 18. The low-speed, high-pressure conditions require a hydrostatic balance because the resulting vane assembly centrifugal loading is not sufficient to provide overall stability. A hydrostatic balance therefore provides vane stability over a wider range of pump speeds and pressures.

The two-piece stepped vane configuration used in the final experimental pump provides the required undervane pressure distribution for both the pumping and the sealing lap spaces. As indicated in Figure 18, the bearing pad hydrostatic pressure profile is not the same for both lap spaces, because high pressure precedes the vane tip on the pumping lap space but trails it on the sealing lap space. In addition, the bearing film profile is not symmetrical about the tip center line, but has its position of minimum film thickness approximately 75 percent of the tip width behind the leading edge ($\frac{x}{B} = .75$). It is therefore necessary to provide a different undervane pressure distribution for each lap space.

To provide a complete balance of the radial hydrostatic forces, the sealing lap space conditions require that 50 percent of the undervane area be subjected to outlet pressure, with the remaining area at inlet pressure. For the pumping lap space conditions, a split of 67 percent at outlet pressure and 33 percent at inlet pressure is required. On

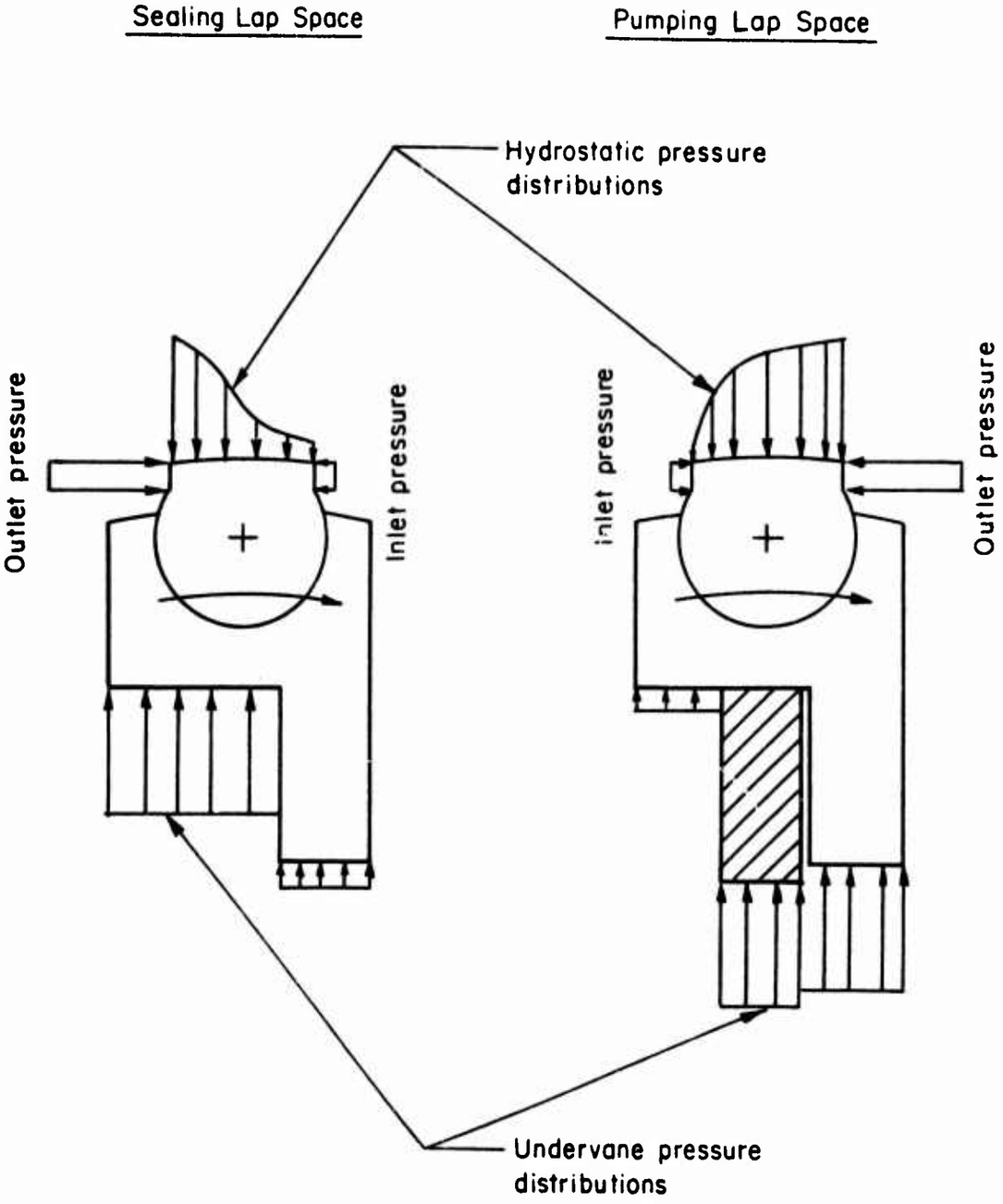

Figure 18. Vane and Vane Tip Hydrostatic Pressure Distributions.

the pumping lap space, this is controlled by the split in the rotor slot; on the sealing lap space, by the split on the stepped vane. The floating vane provides the mechanism by which the undervane distribution is varied. The direction of the pressure differential across this part positions the floating vane as shown in Figure 1 on each lap space so that the proper percentage of undervane area is exposed to outlet pressure.

RESULTS OF VANE ASSEMBLY PERFORMANCE ANALYSIS

The significance of the relative surface profile between the bearing pad and the cam ring is demonstrated in Figure 19. The two curves shown give the tip load capacity versus minimum film thickness for the two radii used to generate the cam ring profile in the experimental fuel pump. The tip pad radius was chosen so that the load capacity on the 0.30-inch cam ring radius is optimized when the operating minimum film thickness is in the 25- to 60-μin. range at 50,000 rpm. The load variable under these conditions ranges from 0.141 to 0.156; the latter value is approximately the theoretical maximum for a centrally pivoted pad bearing. To obtain this optimized condition for a pad width (B) of 0.060 inch, a tip pad radius of 0.295 inch was required. The results on the 0.32-inch cam ring radius are far from optimized, however, as a comparison of the two curves demonstrates. The load variable at a 25 μin. minimum film thickness on the 0.32-inch radius is reduced to 0.038. There is also a marked reduction in the stiffness of the bearing under the unoptimized operating conditions. Therefore, only a very slight variation in cam ring radius is required to reduce the tip load support a considerable amount.

The sensitivity of the bearing design to the relative radii can be reduced by decreasing the pad width (B). This is not a universal solution, however, for the load support is proportional to the square of B as pointed out in equation (2). As a result, it is necessary to compromise the sizing of the tip so that adequate load support is obtained with a realistic variation in cam ring radii.

The above considerations were the basis for the design of the present single-lobe cam ring profile. A stroke of 0.020 inch appeared to be a practical minimum for a high-speed fuel pump and the resulting 0.020-inch variation in cam ring radii appeared to be a practical maximum for sufficient tip load capacity at all operating conditions. A smaller pad width would have allowed for greater pump stroke and would have lowered the vane assembly centrifugal loading, but the resulting load capacity would have required that a minimum film thickness of less than 20 μin. be maintained for 50,000-rpm operation. This appeared to be impractical, for the resulting part surface finish requirements that would allow noncontacting operation would have been extremely demanding.

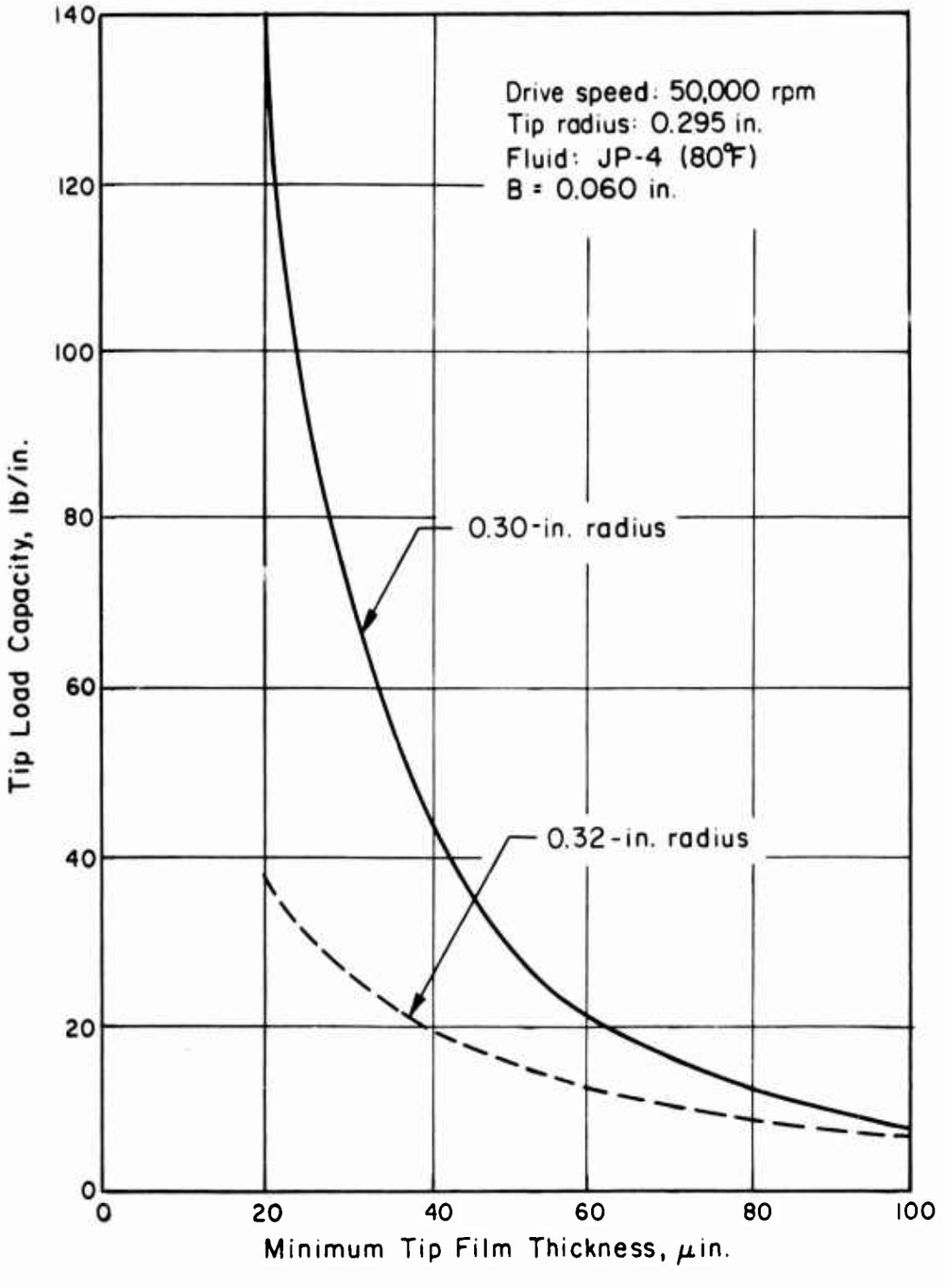

Figure 19. Significance of Surface Profile on Tip Load Capacity.

Curves showing the net tip load capacity versus minimum film thickness at various speeds are given in Figures 20, 21 and 22 for the final experimental pump design. These curves give the load capacity available to support the vane assembly centrifugal loading. The effect of the hydrostatic pressure forces has been included in the results for both lap spaces. The curves represent points of stable equilibrium for both the tip and the vane assembly.

The centrifugal loadings for the various vane operating positions are given in Table VIII for the speeds used in the previous figures. The loading per unit length is increased in the port areas to account for the shorter load-supporting length of the cam ring in these positions. Fifty percent of the length is removed for radial porting on the 0.030-inch radius in both ports, while twenty-five percent is removed on the 0.32-inch radius. Most of the porting is accomplished on the 0.30-inch radius because of the superior load capacity in this portion of the ports.

On the pumping lap space, 67 percent of the undervane area is subjected to outlet pressure, resulting in a hydrostatic radial balance. The sealing lap space was designed with 64 percent of the undervane area exposed to outlet pressure. This exposure results in a radially outward hydrostatic unbalance, but it insures tip stability at the 6000-rpm operating conditions. The need for the unbalance on the sealing lap space is shown in Table IX, which gives the predicted operating film thickness and rotational position of the tip for all vane operating conditions analyzed with the computer. It is arranged to give these parameters for steady-state operation as a vane assembly progresses through one complete pumping cycle. As a vane leaves the outlet port at 6000 rpm, 200 psig, it has a 150-μin. film thickness. On the sealing lap space, however, the tip does not have rotational stability at film thicknesses greater than 75 μin. To insure that operation occurs in the stable range, the vane assembly is forced radially outward by the hydrostatic unbalance. This requires a smaller film thickness to carry the additional loading and places the tip within the stability range. The same type of problem is not encountered of the pumping lap space because the tip has rotational stability at much larger film thicknesses when the high pressure is ahead of it.

Table IX points out that the minimum film thickness of 30 μin. occurs at 50,000 rpm on the 0.32-inch radius of the inlet and outlet ports. At this speed, the tip is predicted to operate with a 30- to 45-μin. range of film thicknesses during each complete pumping cycle. The point of the minimum film thickness varies only slightly during the cycle, however. The slight variation indicates that the tip is basically operating under steady-state conditions, with the effects of transients minimized. It makes the predictions obtained from the steady-state computer analysis more accurate.

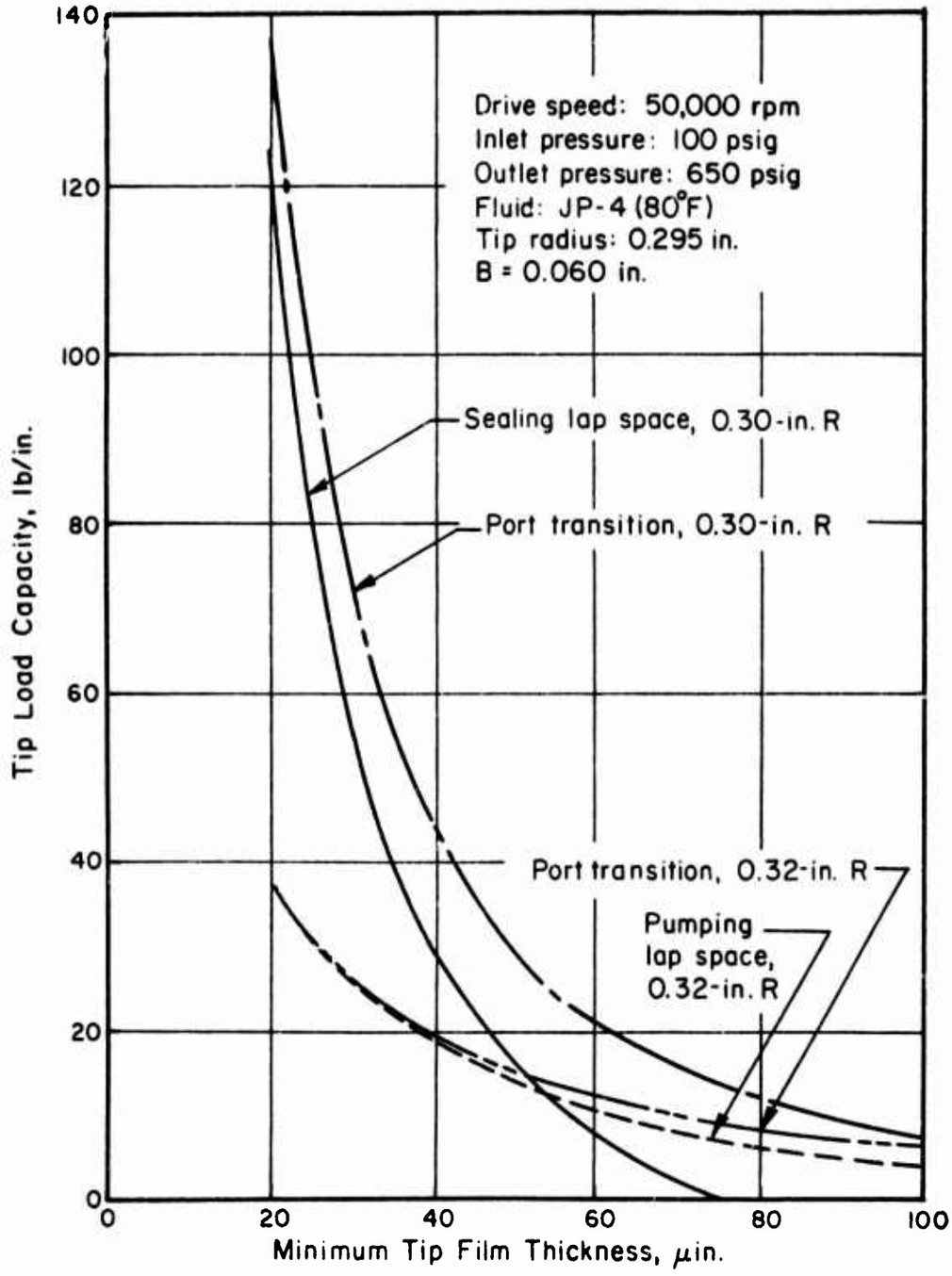

Figure 20. Theoretical Vane Tip Load Capacity - 50,000 RPM.

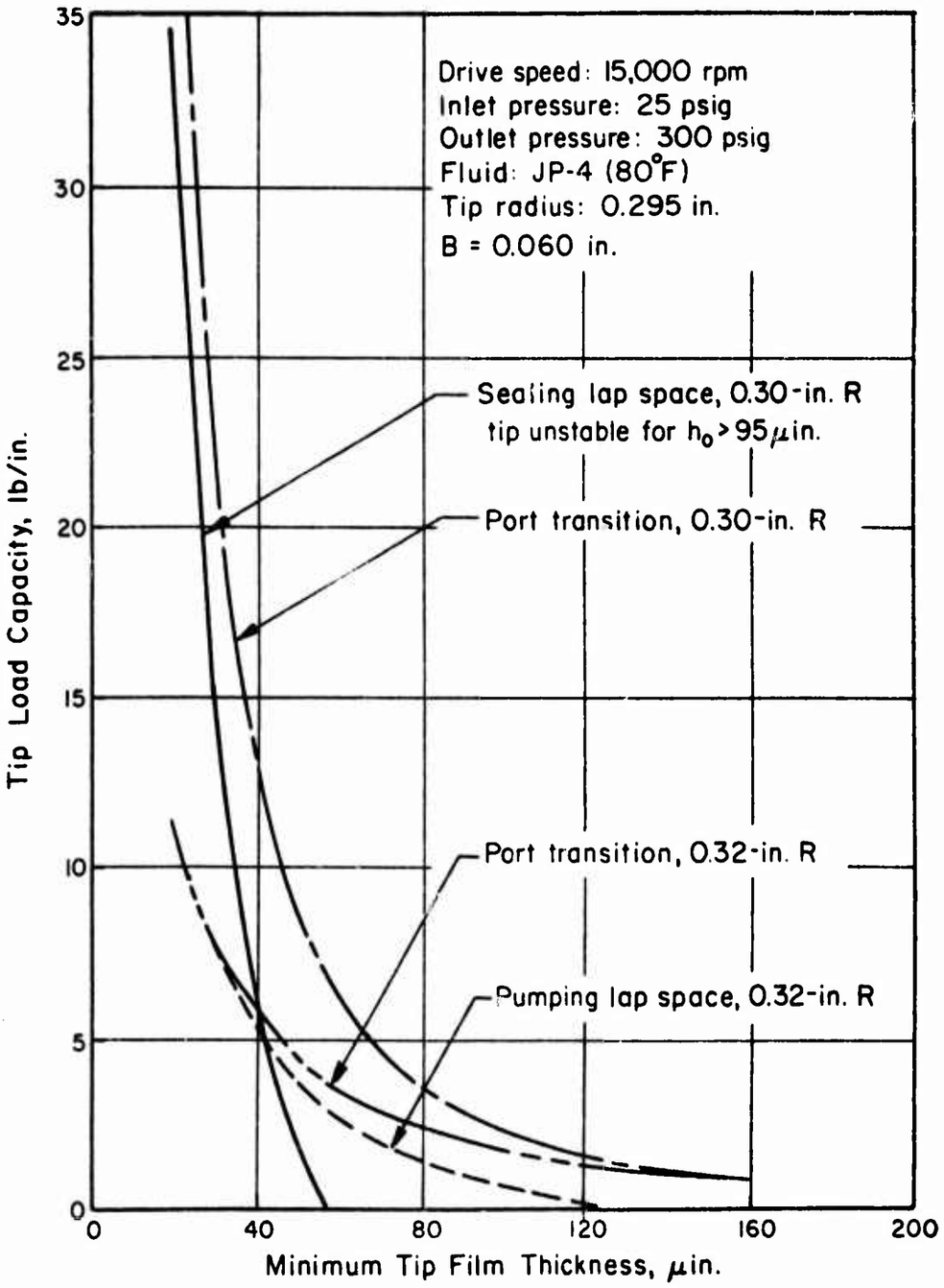

Figure 21. Theoretical Vane Tip Load Capacity - 15,000 RPM.

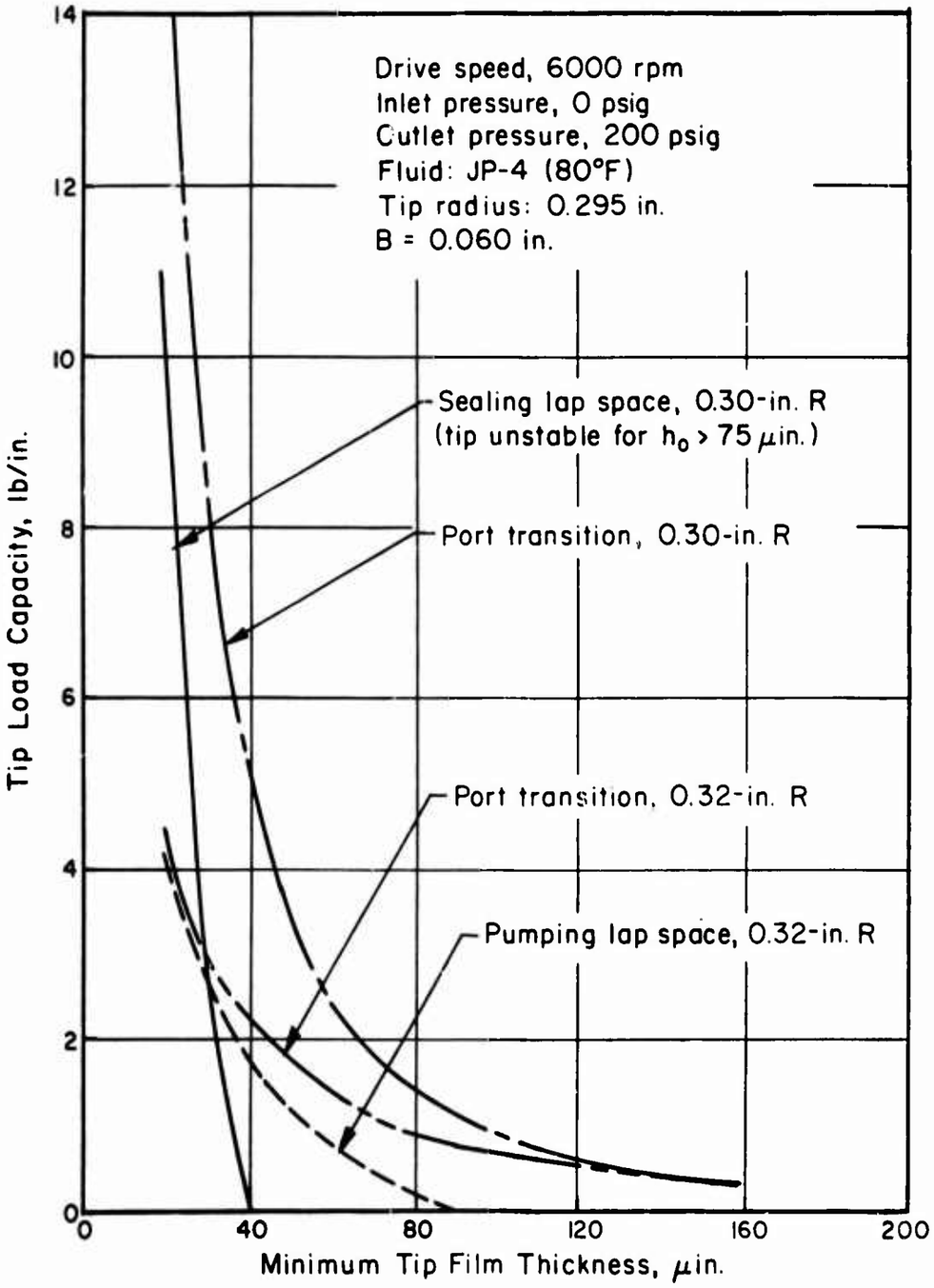

Figure 22. Theoretical Vane Tip Load Capacity - 6000 RPM.

TABLE VIII. VANE ASSEMBLY CENTRIFUGAL LOADING - LB/IN.*

Operating Position	Rotor RPM		
	50,000	15,000	6,000
Sealing Lap Space	18.5	1.7	0.27
0.32 in. Port Transition	24.5	2.2	0.35
0.30 in. Port Transition	43.0	3.9	0.62
Pumping Lap Space	19.5	1.8	0.28

* Loading per inch of cam ring axial length.

TABLE IX. PREDICTED OPERATING FILM THICKNESSES

Operating Position	Rotor RPM					
	50,000		15,000		6,000	
	h_o (μin.)	(x/B) at h_o	h_o (μin.)	(x/B) at h_o	h_o (μin.)	(x/B) at h_o
Sealing Lap Space	45	.77	50	.76	40	.74
0.32 in. Inlet Port Transition	30	.76	85	.76	150	.76
0.30 in. Inlet Port Transition	40	.77	75	.82	120	.86
Pumping Lap Space	37	.76	75	.77	80	.79
0.30 in. Outlet Port Transition	40	.77	75	.82	120	.86
0.32 in. Outlet Port Transition	30	.76	85	.76	150	.76
Sealing Lap Space	45	.77	50	.76	40	.74

Larger film thicknesses are expected for low-speed operation except on the sealing lap space. In the latter case, they actually decrease as speed is decreased due to the hydrostatic radial unbalance required to allow for tip stability. Load support is adequate in this area, however, because the tip operates under optimized conditions by being matched with the 0.30-inch cam ring radius.

APPENDIX II
LUBRICATION AND HYDRAULIC PUMP CONSIDERATIONS

The hypothetical requirements for lubrication and hydraulic pumps that this study is based on are given in Table X. Both of these pumps have flow requirements in the same range as the experimental fuel pump at the 50,000-rpm operating conditions. The fluid used in each pump also has a viscosity level that is of the same order of magnitude as the turbine fuels at the expected operating temperatures. The viscosity may be three or four times greater than with turbine fuels, but the same problems that occurred in the fuel pump design due to low-viscosity fluids can be expected to have a major effect on the design of these two pumps.

HYDRAULIC PUMP

This pump has two additional requirements that make the feasibility of using the fuel pump concepts difficult to evaluate: the variable-displacement requirement and the 4000-psig outlet pressure. To adapt the pivoting tip concept to a high-speed, vane-type fuel pump, it was necessary to use a hydrostatically unbalanced single-lobe design. At outlet pressures above 1500 psig, the single-lobe design becomes much less attractive due to the increased side loading that must be accepted by the pump bearings. A circular, eccentric cam ring profile would produce a reasonably straightforward variable-displacement mechanism. In fact, the single cam ring radius would allow the tip pad radius to be optimized at all positions during the complete pumping cycle and permit an increase in the amount of vane stroke. The rotor, however, would need to be small in diameter and short in axial length so that the area exposed to high pressure and the resulting side loading are minimized. The resulting pump would appear to be best suited for low flow applications; but as a result of this and the high pressure, it would probably have a low volumetric efficiency. At best, the straight utilization of the fuel pump as a high-pressure, variable-displacement hydraulic pump appears to result in a pump of limited application.

A more universally attractive design would be a hydrostatically balanced two-lobe configuration. Research in this area has been done by the Battelle Columbus Laboratories for the Air Force Aero Propulsion Laboratory at Wright-Patterson Air Force Base. The emphasis of this program was placed on the development of a similar hydraulic pump operating at 30,000 rpm and with a capacity of 50 gpm at 4000 psig. A flexible, two-lobe, cam ring concept was used to provide for variable displacement in addition to the use of the pivoting vane tip concept.

This effort has not yet produced hardware that demonstrates the required operating characteristics. It has, however, provided considerable information about the limitations of the design concepts as applied to a pump

TABLE X. LUBRICATION AND HYDRAULIC PUMP REQUIREMENTS

Hydraulic Pump	
Maximum speed:	50,000 rpm
Maximum flow rate:	5 gpm (variable displacement required)
Design pressure at 100 percent speed:	4000 psig
Hydraulic fluid:	MIL-H-5606
Fluid inlet temperature:	250° to 300°F
Lubrication Pump	
Maximum speed:	50,000 rpm
Flow rate at 100 percent speed:	3 gpm
Flow rate at 60 percent speed:	2 gpm
Design pressure at 100 percent speed:	40 to 100 psig
Design pressure at 60 percent speed:	20 to 50 psig
Lubrication oil:	MIL-L-7808 or MIL-L-23699
Fluid inlet temperature:	300°F maximum

of this type. The effects of a low-viscosity fluid in combination with the difficulty in obtaining the proper cam ring profile to provide tip load capability and stability leave the feasibility of the pump experimentally as yet undetermined.

The Battelle approach to the high tip surface speeds resulting from high rotational speeds has been the use of the hydrodynamically lubricated pivoting vane tip. Research to date indicates that although this approach provides a theoretical advantage, a compromise of the hydraulic aspects of the pump design appear to be necessary to obtain proper mechanical operation of the tip with low viscosity fluids and high differential pressures. The small, 0.020-inch fuel pump stroke is the result of such a compromise.

A two-lobe cam ring profile produces a large variation in radius of curvature, particularly as the stroke is increased. A high-speed pump also requires a minimization of the rotor diameter to reduce the charging pressure necessary to accelerate the fluid to vane tip velocity without cavitation at the inlet. Both these factors produce conditions which detract from the theoretical requirements necessary to produce the proper relative surface profile between the tip pad and the cam ring. Therefore, the high-speed capability of the tip and its ability to achieve stable equilibrium when exposed to high differential pressures are severely penalized.

By increasing the diameter and reducing the vane stroke, the feasibility of proper tip operation is increased. The hydraulic characteristics of the pump would then be penalized, particularly the overall efficiency under high-pressure operating conditions. Operation of a 1.5-inch-rotor-diameter pump at 50,000 rpm would require a minimum of 600 psi at the pump inlet, and this requirement is unattractive. Yet, this diameter combined with a maximum stroke of 0.020 inch would provide a favorable relative surface profile between the tip pad and cam ring.

Because of the conflicting design requirements noted above, it appears that the pivoting vane tip concept may have feasibility only in certain vane pump applications. Use of a solid vane operating with high tip speeds and with boundary lubrication has not been thoroughly investigated during the Battelle research to date. The proper selection of vane and cam ring materials will probably determine the surface speed limit for these conditions. A design using this technique appears to have less conflict with pump hydraulic requirements, but until the design is thoroughly investigated, a prediction of the speed limitations will be difficult.

A reduction in the 50,000-rpm requirement to the 25,000- to 30,000-rpm range would make the development of the hypothetical hydraulic pump more realistic with the information presently available. The lower speed reduces the charging pressure requirements and makes the vane tip design less critical. The choice of a solid vane versus a vane with a pivoting tip is a difficult one that requires more research for this application. The two-lobe flexible cam ring concept has shown experimental feasibility, but satisfactory manufacturing techniques have not yet been established.

In general, the design of a high-speed, high-pressure hydraulic pump appears to be feasible. The potential capabilities of such a pump have not been established. It is hoped that further research will better define the speed and pressure limits and provide more information about the efficiencies to be expected. With this information, the potential of the present concepts can be more fairly evaluated.

LUBRICATION PUMP

The low-pressure requirements of this pump at the maximum speed make the use of a high-speed positive-displacement pump very unattractive. The inlet pressure requirements at 50,000 rpm would be at least 50 psig, even for a 0.5-inch-diameter rotor. This is approximately identical to the required outlet pressure. It would appear that a small centrifugal pump of the type used for the fuel pump charging stage would provide adequate discharge pressure at 50,000 rpm, even for outlet pressures up to 200 psig. The major problem would be a need to maintain pressure at the light-off speed conditions. The developed head of a centrifugal pump decreases in proportion to the square of the speed and the pump would develop very little at 10 percent of maximum speed. This requirement appears unlikely, however.

A direct utilization of the fuel pump concepts would appear practical only where outlet pressures above 300 psig are required and when the pressure must be maintained over a wide range of speeds.

APPENDIX III
FEASIBILITY OF UTILIZING AN EMULSIFIED FUEL

The information available on the present emulsified fuels[6,7] indicates that the emulsions will break down to the liquid form when subjected to high shear rates and recirculation through pumping devices. The preliminary studies showed that fuel emulsions can be pumped by low-speed, high-capacity pumps without changing their state. High-speed, low-capacity pumps produced considerable breakdown.

Based on this information, it appears that the high-speed experimental fuel pump would cause at least partial recovery of the liquid fuel by pumping the emulsion. It is very likely that the centrifugal stage would cause complete liquid fuel recovery at the centrifugal outlet due to the high speed and the high level of recirculation that takes place within this stage at present. Therefore, if no breakdown of the emulsion is a requirement, a high-speed pump appears to be impractical.

If breakdown of the emulsion at this point in the flow path to the turbine nozzles is acceptable, then it appears that pumping the emulsion with the experimental fuel pump is feasible. This is particularly true if complete emulsion breakdown occurs within the less sensitive centrifugal stage. The vane pump stage would be supplied with liquid fuel under these conditions and should not show any changes in its overall pumping characteristics.

If partial liquid recovery is obtained in the centrifugal stage, the resulting liquid-emulsion combination may present problems in the vane pump stage. The abilities of the pivoting vane tip may be degraded due to the presence of the emulsion, but only an experimental evaluation could provide a firm answer. The effects of the emulsion clogging the undervane areas and tip socket area could also produce potential problems. The presence of the emulsion may be unimportant at the higher operating speeds where considerable liquid recovery can be expected in the centrifugal stage. At the low-speed, light-off conditions, however, the emulsion may create difficulties.

The preliminary studies[6,7] indicated that the emulsions can be readily pumped, but they do not necessarily flow well into the pump inlet. The poor inlet flow results in pump cavitation, which could be an increased problem with the high-speed fuel pump. A high-speed pump is much more sensitive to low inlet pressures, and the use of an emulsion may create additional difficulties. Flow problems between the centrifugal and vane stages may also present a potential problem because of the small passages. The experimental pump has a wide safety margin in charging the vane pump stage, but improvements in the overall efficiency may not be possible if this margin is maintained to insure proper flow of the emulsified fuel.

The use of the emulsified fuels would require that the pump be able to accept much higher than normal levels of contamination due to filtration problems. The effects of corrosion may also increase with the use of a water emulsion. Both of these additional problems are concerned with materials selection in the pump, and verification of the pump's abilities can only be determined experimentally. The effects of contamination will definitely be the most difficult to eliminate. Contamination may have both short-and long-term effects, depending on the contaminant particle size.

Unclassified
Security Classification

DOCUMENT CONTROL DATA - R & D

(Security classification of title, body of abstract and indexing annotation must be entered when the overall report is classified)

1. ORIGINATING ACTIVITY (Corporate author) Battelle Memorial Institute, Columbus Laboratories 505 King Avenue Columbus, Ohio 43201	2a. REPORT SECURITY CLASSIFICATION Unclassified 2b. GROUP

3. REPORT TITLE

Advanced High-Speed Fuel Pumps for Small Gas-Turbine Engines

4. DESCRIPTIVE NOTES (Type of report and inclusive dates)

Final Technical Report

5. AUTHOR(S) (First name, middle initial, last name)

Harry T. Johnson

Robert K. Mitchell

6. REPORT DATE	7a. TOTAL NO. OF PAGES	7b. NO. OF REFS
April 1969	86	13

8a. CONTRACT OR GRANT NO.	9a. ORIGINATOR'S REPORT NUMBER(S)
DAAJ02-67-C-0037 b. PROJECT NO. Task 1G162203D14416 c. d.	USAAVLABS Technical Report 69-12 9b. OTHER REPORT NO(S) (Any other numbers that may be assigned this report)

10. DISTRIBUTION STATEMENT

This document has been approved for public release and sale; its distribution is unlimited.

11. SUPPLEMENTARY NOTES	12. SPONSORING MILITARY ACTIVITY
	U.S. Army Aviation Material Laboratories Ft. Eustis, Virginia

13. ABSTRACT

The object of this program was to develop the technology necessary for vane-pump operation at turbine rotational speeds. Major hardware emphasis was devoted to the evaluation of a high-speed fuel pump based upon this technology. A single-lobe vane pump with a centrifugal charging stage has been designed and successfully operated at 40,000 rpm pumping JP-4 turbine fuel. The vane pump relies upon the use of a hydrodynamically lubricated pivoting vane tip to support vane assembly radial loading. The hydrodynamic film allows a significant increase in tip surface speed without sacrificing the required endurance life. A 200-hour endurance run at speeds from 24,000 to 40,000 rpm has been successfully completed with no noticeable performance degradation. Successful contamination experiments were performed after completion of 175 hours of the endurance schedule. The contamination experiments were not extensive, but they verified that the design concepts were not unduly sensitive to contaminated fuel. Continued development will be required to establish life capability at the design pressure of 650 psig, but short-term capability has been established at outlet pressures up to 600 psig. No major limitations with the basic pump design have been found. The 50,000-rpm goal appears to be feasible, but further evaluation at speeds above 40,000 rpm was terminated due to bearing problems in the laboratory speed-increaser system.

DD FORM 1 NOV 68 1473 REPLACES DD FORM 1473, 1 JAN 64, WHICH IS OBSOLETE FOR ARMY USE.

Unclassified
Security Classification

14. KEY WORDS	LINK A		LINK B		LINK C	
	ROLE	WT	ROLE	WT	ROLE	WT
pump						
vane						
centrifugal						
fuel						
high-speed						
turbine-speed						
single-lobe vane pump						
pivoting-tip vane						
centrally pivoted pad bearings						
hydrodynamic lubrication						
stepped vane						
floating vane						

3394-69